Chemical Communications

Electronic Supplementary Information (ESI)

Highly-efficient dye-sensitized solar cells with collaborative sensitization by silyl-anchor and carboxy-anchor dyes

Kenji Kakiage,[a] Yohei Aoyama,[a] Toru Yano,*[a] Keiji Oya,[a] Jun-ichi Fujisawa[b] and Minoru Hanaya*[b]

[a] Environmental & Energy Materials Laboratory, ADEKA CORPORATION, 7-2-35 Higashiogu, Arakawa, Tokyo 116-8554, Japan.

[b] Division of Molecular Science, Graduate School of Science and Technology, Gunma University, 1-5-1 Tenjin-cho, Kiryu, Gunma 376-8515, Japan.

Corresponding authors
    Minoru Hanaya[b] (mhanaya@gunma-u.ac.jp)
    Toru Yano[a] (yanotoru@adeka.co.jp)

Chemical Communications

Electronic Supplementary Information (ESI)

a) Photosensitizing dyes used in this work:

A carbazole/hexyl-functionalized oligothiophene/trimethoxysilyl-anchor dye (**ADEKA-1**) was synthesized by using **MK-2**[1] as a starting material.[2,3] Dibiphenylmonophenylamine dyes (**LEG4** and **D35**) were purchased from Dyenamo and a triphenylamine dye (**L0**) was synthesized by using the general method.[4-7] An indoline dye (**D131**) was purchased from Mitsubishi Paper Mills.[8] Molecular structures of these photosensitizing dyes are shown in Fig. S2.

b) Device fabrication of Cell-A:

The Cell-A is the cell for checking photosensitization properties of the dyes. The nanocrystalline porous TiO_2 film electrodes were prepared by squeegeeing a commercial TiO_2 paste [JGC Catalysts and Chemicals, PST-18NR[9]] on the washed F-doped SnO_2 (FTO)-coated glass plates (9-11 Ω/sq.; Asahi Glass) followed by sintering the TiO_2 layers at 450 °C. The thickness of the transparent porous TiO_2 film was estimated to be ~4 μm. An adsorption of **ADEKA-1** on the TiO_2 electrodes was performed by immersing the electrodes in a toluene solution with 3.0×10^{-4} M **ADEKA-1** at ~25 °C for 2 h, and then the dye-adsorbed electrodes were washed with toluene and ethanol. Adsorptions of the other photosensitizing dyes (**LEG4**, **D35**, **L0** and **D131**) on the TiO_2 electrodes were performed by immersing the electrodes in ethanol solutions with 3.0×10^{-4} M dyes at ~25 °C for 2 h, and then the dye-adsorbed electrodes were washed with ethanol. Co-adsorptions of the dyes (**LEG4**, **D35**, **L0** and **D131**) on the **ADEKA-1**-adsorbed TiO_2 electrodes were carried out by immersing the **ADEKA-1**-adsorbed electrodes in the ethanol solutions containing 3.0×10^{-4} M dyes at ~25 °C for 2 h, and then the electrodes were washed with ethanol. Before the immersion in the **ADEKA-1** solution, the TiO_2 electrodes were kept in air at 120 °C for 2 h to eliminate adsorbed water on the TiO_2 surface for the efficient dye adsorption.

Photovoltaic measurements were performed for the electrochemical cells of an open sandwich type. A platinum-deposited stainless-steel plate was employed as the counter electrode and a solution with I_3^-/I^- (0.50 M LiI, 0.05 M I_2 in MeCN) was used as the redox electrolyte solution. The dye-adsorbed TiO_2 electrode, the counter electrode and a polyethylene film spacer with ~40 μm thick were assembled into a cell, and the redox electrolyte solution was injected into the space between the electrodes.

c) Device fabrication of Cell-B:

The Cell-B is the cell for a high photovoltaic performance. The nanocrystalline porous TiO_2 film electrodes were prepared on the UV-O_3, $TiCl_4$ and $Nb(OC_4H_9)_5$-treated FTO-coated glass plates (9 Ω/sq.; Nippon Sheet Glass) by spin-coating and screen-printing methods with subsequent sintering at 520 °C.[10,11] The commercial TiO_2 powders (Nippon Aerosil, Ishihara

Sangyo Kaisha, Tayca Corporation and JGC C&C) were used with purifications. The thickness of the porous TiO_2 film with the multilayer structure was estimated to be ~10 μm (blocking layer ~ 0.2 μm, transparent layer ~ 4 μm, semitransparent layer ~ 2 μm and scattering layer ~ 4 μm). Then, the surface of the TiO_2 electrodes were modified by the $TiCl_4$, $Al[OCH(CH_3)_2]_3$ and $Mg(OC_2H_5)_2$ treatments to prevent the back-electron transfer.[10,12] An adsorption of **ADEKA-1** on the TiO_2 electrodes was performed by immersing the electrodes in a toluene-acetonitrile (9:1 in volume) solution with 2.0×10^{-4} M **ADEKA-1** and 1.0×10^{-4} M coadsorbent of isooctyltrimethoxysilane (Gelest) at 10 °C for 15 h, and then the dye-adsorbed electrodes were washed with toluene, acetonitrile and ethanol.[2,3] A co-adsorption of **LEG4** on the **ADEKA-1**-adsorbed TiO_2 electrodes was carried out by immersing the **ADEKA-1**-adsorbed electrodes in the ethanol solution containing 3.0×10^{-4} M **LEG4** at 25 °C for 2 h, and then the **ADEKA-1** + **LEG4**-co-adsorbed electrodes were washed with ethanol and acetonitrile. Before the immersion in the **ADEKA-1** solution, the TiO_2 electrodes were treated with UV-O_3, heated in air at 100 °C for 5 h and then cooled to 80 °C to eliminate adsorbed water on the TiO_2 surface for the efficient dye adsorption. The hierarchical multi-capping treatment was performed to the **ADEKA-1** + **LEG4**-co-adsorbed TiO_2 electrodes by immersing the electrodes in a 1.0×10^{-4} M toluene-acetonitrile (3:2 in volume) solution at 25 °C of octadecylphosphonic acid (ODPA) for 1 min and in 1.0×10^{-3} M toluene-acetonitrile (1:1 in volume) solutions at 25 °C of octadecyltrimethoxysilane (ODTMOS) for 10 min, dodecyltrimethoxysilane (DDTMOS) for 10 min, octyltrimethoxysilane (OTMOS) for 10 min, isooctyltrimethoxysilane (IOTMOS) for 10 min and ethyltrimethoxysilane (ETMOS) for 15 min in turn to form the 'alkyl-thicket' structure on the TiO_2 photoelectrodes (Figs. S19 and S20).[2,3]

Photovoltaic measurements were performed for the electrochemical cells of an open sandwich type. A platinum-deposited FTO-coated glass plate (FTO/Pt), which was prepared by a rf magnetron sputtering of Pt and the reported H_2PtCl_6 treatment,[13] and graphene nanoplatelets (GNP) + gold-treated FTO-coated glass plate (FTO/Au/GNP), which was prepared by a vacuum evaporation of Au and the reported GNP treatment,[14,15] were employed as the counter electrodes. The mixture (1:1 in weight) of a commercial graphene (Cheap Tubes, Grade 3: t ~ 8 nm, d < ~2 μm) and an exfoliated graphene (t ~ 5 nm, d < ~5 μm) prepared by ADEKA was employed as the GNP. As for the redox electrolytes, six redox electrolyte solutions with I_3^-/I^- or cobalt(III/II) complexes were used: A) 0.07 M I_2, 0.05 M LiI, 0.05 M NaI, 0.50 M 1,2-dimethyl-3-*n*-propylimidazolium iodide (DMPImI), 0.10 M 1-ethyl-3-methylimidazolium iodide (EMImI), 0.05 M tetra-*n*-butylammonium iodide (TBAI), 0.05 M tetra-*n*-hexylammonium iodide (THAI), 0.40 M 4-*tert*-butylpyridine (TBP), 0.10 M 4-methylpyridine (MP), 0.10 M guanidinium thiocyanate (GuSCN) in MeCN/valeronitrile (VN)/tetrahydrofuran (THF) (8:1:1 in volume) (Fig. S21),[16-19] B) 0.25 M $[Co^{2+}(phen)_3](PF_6^-)_2$, 0.035 M $[Co^{3+}(phen)_3](PF_6^-)_3$, 0.10 M $LiClO_4$, 0.50 M TBP in MeCN,[20] C) 0.20 M $[Co^{2+}(phen)_3](PF_6^-)_2$, 0.05 M $[Co^{3+}(phen)_3](PF_6^-)_3$, 0.10 M $LiClO_4$, 0.50 M TBP in MeCN, D) 0.20 M $[Co^{2+}(phen)_3](TFSI)_2$, 0.05 M $[Co^{3+}(phen)_3](TFSI)_3$, 0.10 M $LiClO_4$, 0.50 M TBP in MeCN, E) 0.20 M $[Co^{2+}(phen)_3](PF_6^-)_2$, 0.05 M $[Co^{3+}(phen)_3](PF_6^-)_3$, 0.07 M $LiClO_4$, 0.02 M $NaClO_4$, 0.03 M tetrabutylammonium hexafluorophosphate (TBAPF), 0.01 M tetrabutylphosphonium hexafluorophosphate (TBPPF), 0.01 M 1-hexyl-3-methylimidazolium hexafluorophosphate (HMImPF), 0.30 M TBP, 0.10 M 4-trimethylsilylpyridine (TMSP),[21] 0.10 M MP in MeCN,[2,3] F) 0.20 M $[Co^{2+}(phen)_3](PF_6^-)_2$, 0.05 M $[Co^{3+}(phen)_3](PF_6^-)_3$, 0.07 M $LiClO_4$, 0.02 M $NaClO_4$, 0.03 M TBAPF, 0.01 M TBPPF, 0.01 M HMImPF, 0.30 M TBP, 0.10 M TMSP, 0.10 M MP, 0.05 M 4-cyano-4'-propylbiphenyl (CPrBP), 0.10 M 4-cyano-4'-pentylbiphenyl (CPeBP), 0.05 M 4-cyano-4'-octylbiphenyl (COcBP) in MeCN (Fig. S22).[22]

The dye-adsorbed TiO_2 electrode, the counter electrode and a polyethylene film spacer with ~12 μm thick were assembled into a cell, and the redox electrolyte solution was injected into the space between the electrodes.

d) Photovoltaic measurements:

The photovoltaic performances of the fabricated dye-sensitized solar cells (DSSCs) with an antireflection film were assessed from the incident monochromatic photon-to-current conversion efficiency (*IPCE*) spectra and the photocurrent-voltage (*J-V*) properties of the cells with maintaining the aperture area of the cells to be 0.320 × 0.320 cm^2 by the use of a square black shade mask with 30 μm thick (Bunkoukeiki) (Fig. S23). The *IPCE* spectra were obtained by using a monochromatic light source of SM-25 (Bunkoukeiki) and an electrometer of R8240 (Advantest) at 25 °C. The *J-V* properties were measured by using a solar simulator with Class AAA of OTENTO-SUN III (Bunkoukeiki) and a source meter of R6240A (Advantest) under the simulated sunlight illumination of AM-1.5G one sun condition (100 mW cm^{-2}) at 25 °C. Lower light intensities were also applied. The power of the simulated sunlight was calibrated by the use of a reference Si photodiode for DSSCs of BS-520 (Bunkoukeiki). The *J-V* properties were obtained by applying an external bias to the cells and measuring the generated photocurrent with the source meter. The voltage step and delay time for the photocurrent measurements were set to be 5 mV and 250 ms, respectively.

$$IPCE\ (\%) = \{(1240\ [\mathrm{V\ nm}] \times J_{\mathrm{ph}}\ [\mathrm{mA\ cm^{-2}}]) / (\lambda\ [\mathrm{nm}] \times I_{\mathrm{m}}\ [\mathrm{mW\ cm^{-2}}])\} \times 100$$

J_{ph} is the short-circuit photocurrent density for the monochromatic light irradiation. λ and I_{m} are the wavelength and the intensity of the monochromatic light, respectively.

$$\eta\ (\%) = \{(J_{\mathrm{sc}}\ [\mathrm{mA\ cm^{-2}}] \times V_{\mathrm{oc}}\ [\mathrm{V}] \times FF) / I_{\mathrm{s}}\ [\mathrm{mW\ cm^{-2}}]\} \times 100$$

The overall light-to-electric energy conversion efficiency (η) of the DSSC is determined by the short-circuit photocurrent density (J_{sc}), the open-circuit photovoltage (V_{oc}), the fill factor (*FF*) [= P_{max} / ($J_{\mathrm{sc}} \times V_{\mathrm{oc}}$)] of the cell and the intensity of the incident simulated sunlight (I_{s}). P_{max} is the product of $J_{P\mathrm{max}}$ and $V_{P\mathrm{max}}$, that are photocurrent density and photovoltage at the voltage where the power output of the cell is maximal.

e) Other measurements and calculations:

Optical measurements: The UV-visible absorption spectra of photosensitizing dye solutions were recorded on a HITACHI U-3010 spectrophotometer at ~25 °C. An integrating sphere was equipped to the spectrophotometer for the measurements of the dye-adsorbed TiO_2 electrodes. The emission spectra of photosensitizing dye solutions and Al_2O_3 porous films with **ADEKA-1** and/or **LEG4** were recorded on a JASCO FP-8300 spectrofluorometer at ~25 °C with the excitations at 475 and 500 nm. The semitransparent Al_2O_3 porous films with ~3 μm thick on the FTO-coated glass plates (Asahi Glass) were made of AEROXIDE Alu C (Nippon Aerosil) by the use of a screen printing method.

Molecular orbital (MO) calculations: We optimized the molecular structures and calculated the energy levels of frontier orbitals and others for the trimethoxysilyl carbazole dye (**ADEKA-1**) and the carboxy triarylamine dye (**LEG4**) on the Gaussian 09 program package by using a density functional theory (DFT).[23] A Becke's three-parameter hybrid functional with the LYP correlation functional (B3LYP) and a better hybrid exchange-correlation functional of coulomb-attenuating method-B3LYP (CAM-B3LYP) were employed together with 6-31+G(d,p) basis set.[24-26] Geometry optimizations and calculations of electronic properties of the dyes were performed without any symmetry constraint in the gas phase and by assuming the target molecules to be isolated. Calculated molecular orbitals were visualized by using the Winmoster (X-Ability Co.,Ltd.). In addition, we calculated the lowest 3 singlet transitions of the dyes by using a time-dependent density functional theory (TDDFT) method,[27] and the absorption spectra of the dyes were estimated by applying an artificial Gaussian broadening.

Internal quantum efficiency (*IQE*) measurements: The *IQE* spectra of the cells photosensitized by **ADEKA-1** and/or **LEG4** were estimated by using cells, which were fabricated in the same procedures as Cell-A but changing only the thickness of the TiO_2 films to be ~1 μm, based on a following equation.[28] The hyper monolight of SM-25 (Bunkoukeiki) was used as the monochromatic light source in the measurements.

$$IQE\ (\%) \approx \Phi_{\mathrm{dye}} = (J_{\mathrm{ph}} / e) / \{I \times 10^{-Abs.(\mathrm{TiO2})} \times (1\text{-}10^{-Abs.(\mathrm{Dye})})\}\ ,\ \ I = (W\lambda / hc)$$

Φ_{dye} is the photocurrent generation efficiency (quantum yield). J_{ph} is the short-circuit photocurrent density for monochromatic irradiation, e is the elementary charge, I is the number of photons per unit area and unit time, λ is the wavelength of the light irradiation, *Abs.*(TiO_2) is the absorbance of the TiO_2 electrode, *Abs.*(Dye) is the absorbance of the dyes adsorbed on the TiO_2 electrode, W is the irradiated light power, h is the Planck's constant and c is the light velocity.

Open-circuit voltage decay (OCVD) measurements: The cells photosensitized by **ADEKA-1** with/without **LEG4** (Cell-A) were used to measure OCVDs. The cells were illuminated at an open-circuit condition under the AM-1.5G one sun simulated sunlight (100 mW cm^{-2}) at 25 °C by using the solar simulator (OTENTO-SUN III, Bunkoukeiki). After the open-circuit photovoltages (V_{oc}) indicated steady values, the illumination was turned off with a shutter, and OCVDs were plotted with the measurement step of 200 ms. The lifetimes of the electrons in the TiO_2 conduction band were calculated by using the results of the OCVD measurements based on a following equation.[29]

$$\tau_n = -(k_{\mathrm{B}}T / e) \times (\mathrm{d}V_{\mathrm{oc}} / \mathrm{d}t)^{-1}$$

τ_n is the lifetime of an electron in the TiO_2 conduction band, k_{B} is the Boltzmann constant, T is temperature, e is the elementary charge and t is time after turning off the simulated sunlight.

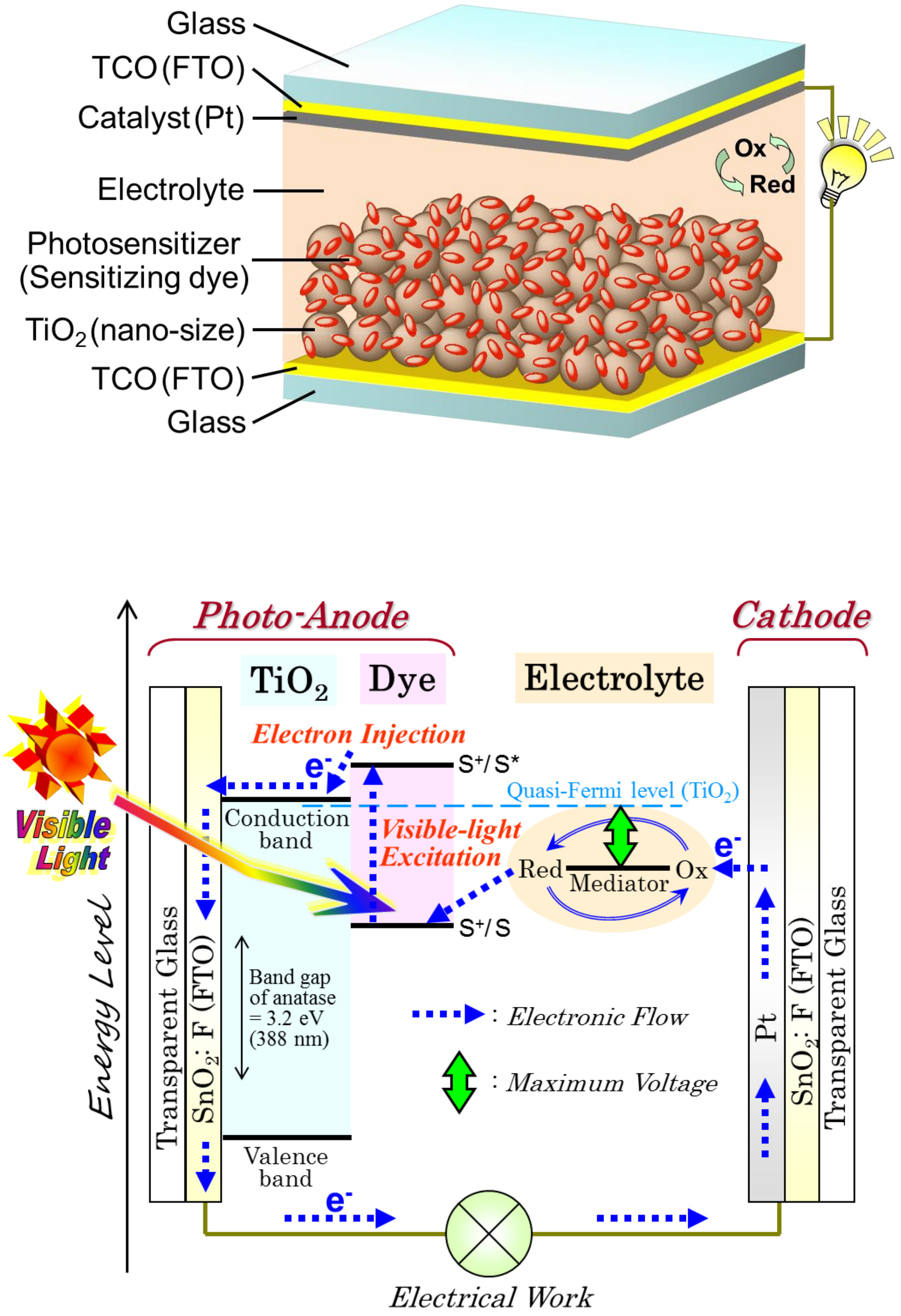

Figure S1. Schematic illustrations of the structure and the operation principle for DSSCs.

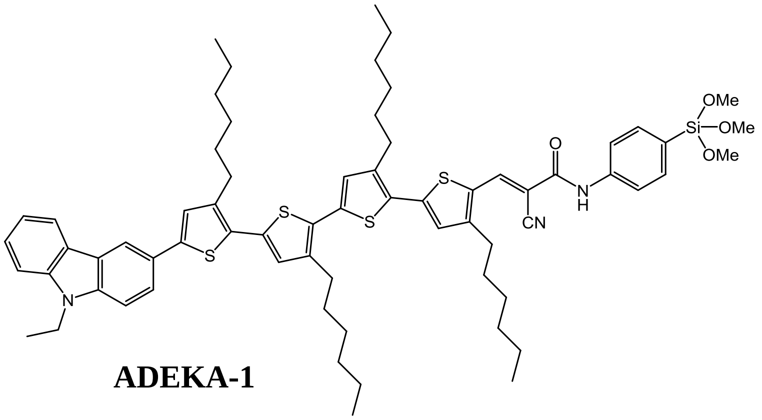

ADEKA-1

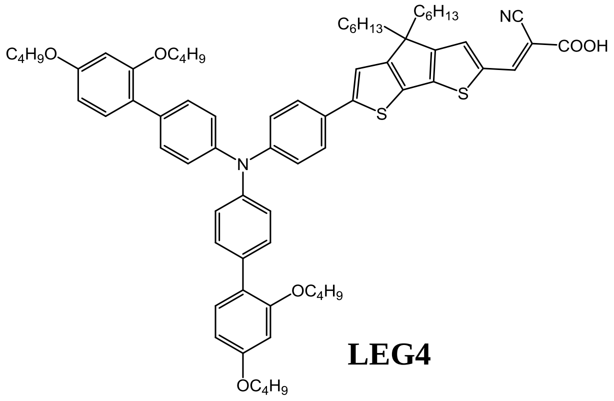

LEG4

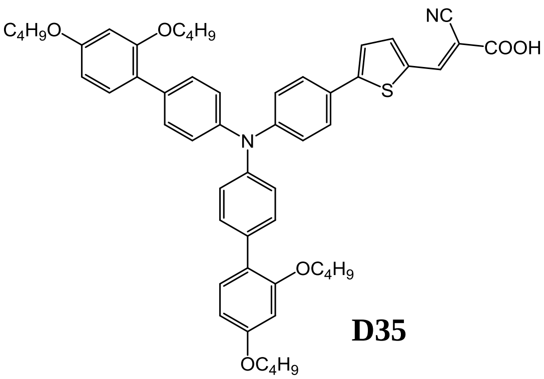

D35

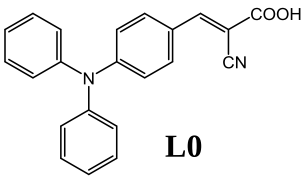

L0

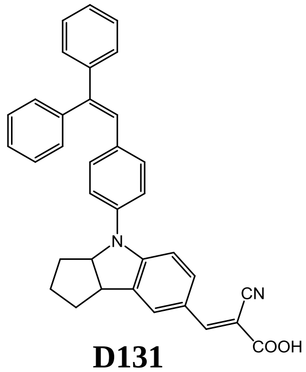

D131

Figure S2. Molecular structures of **ADEKA-1** and the dyes employed as the co-photosensitizers in this work (**LEG4**, **D35**, **L0** and **D131**).

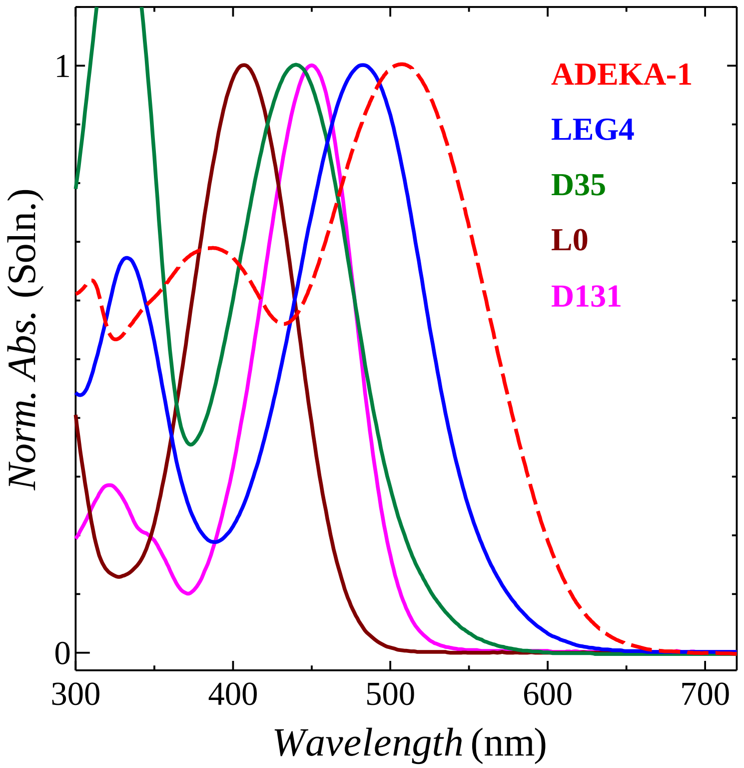

Figure S3. Normalized absorption spectra of the solutions containing **ADEKA-1** and the dyes employed as the co-photosensitizers in this work. Chloroform for **ADEKA-1** and ethanol for the others were used as the solvents.

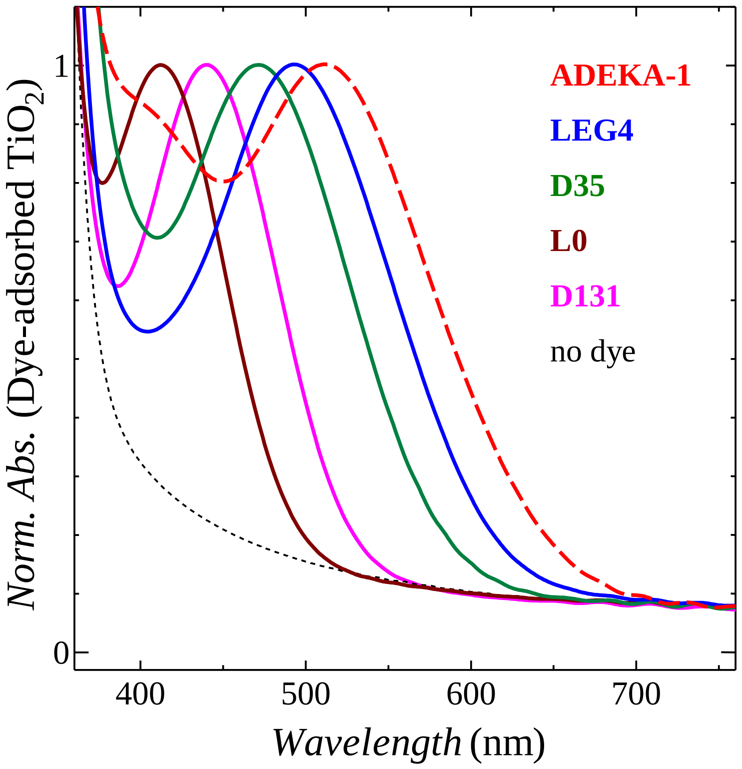

Figure S4. Normalized absorption spectra of the transparent TiO$_2$ films with **ADEKA-1** and the dyes employed as the co-photosensitizers in this work.

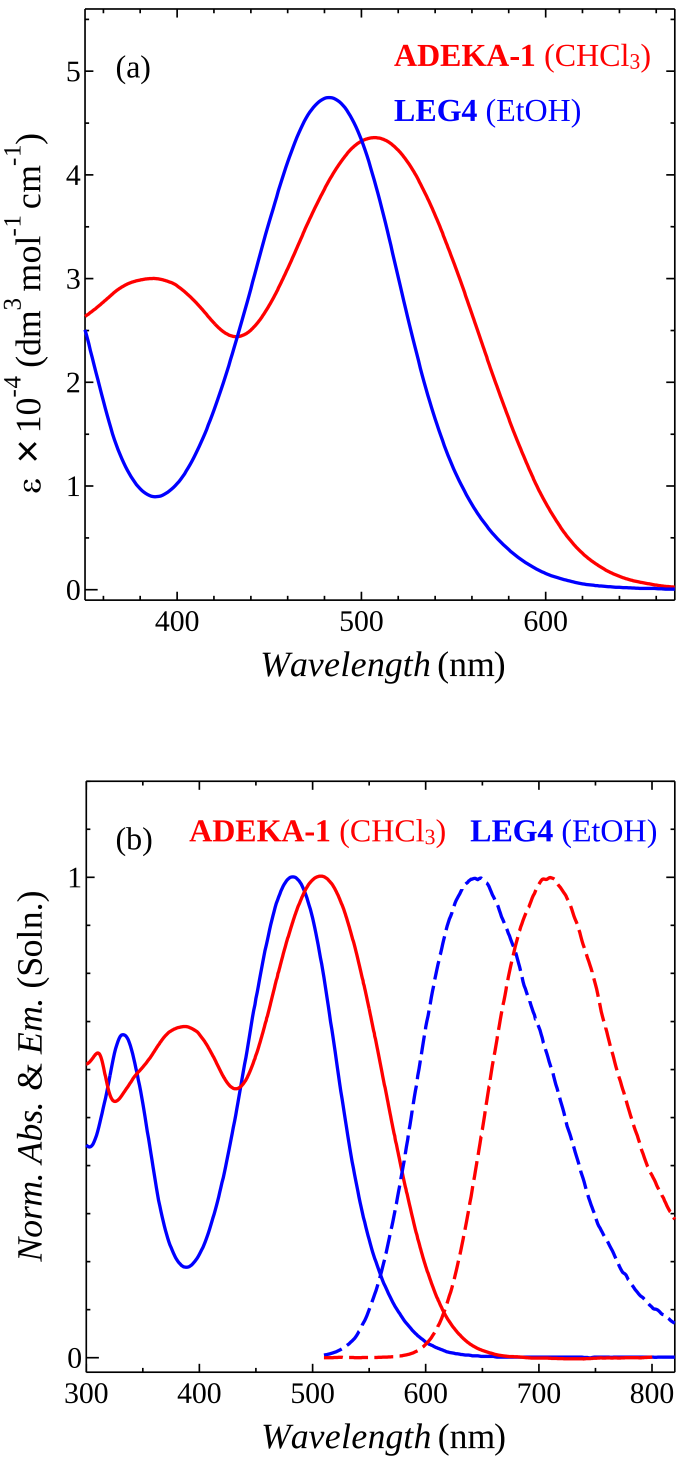

Figure S5. (a) Absorption spectra and (b) normalized absorption spectra (solid lines) and emission spectra with λ_{ex} = 475 nm (dashed lines) of **ADEKA-1** in a chloroform solution and **LEG4** in an ethanol solution.

Table S1. Optical and electrochemical data for **ADEKA-1** and **LEG4**.

Dye	Absorption[a]		Emission[a]	$E_{0\text{-}0}$ (eV)[b]	Potential *vs* NHE[c]		Driving Force[d]	
	λ_{max} (nm)	ε_{max} ($dm^3\ mol^{-1}\ cm^{-1}$)	λ_{max} (nm)	on TiO_2	E_{ox} (V)	E_{ox}^* (V)	$\|\Delta G_{inj}\|$ (eV)	$\|\Delta G_{reg}\|$ (eV)
ADEKA-1	507	43,500	708	1.85	0.99	-0.86	0.36	0.59
LEG4	483	47,500	645	1.91	1.07	-0.84	0.34	0.67

a) Steady-state absorption and emission data were observed by using a chloroform solution of **ADEKA-1** and an ethanol solution of **LEG4**. *b*) Lowest transition energies ($E_{0\text{-}0}$, approximately HOMO-LUMO gaps) were estimated from absorption onsets in the absorption spectra of the dye-adsorbed TiO_2 electrodes (Fig. S4). *c*) Oxidation potentials (E_{ox} *vs*. NHE) are literature values.[2,4] Excited state oxidation potentials (E_{ox}^* *vs*. NHE) were estimated from E_{ox} and $E_{0\text{-}0}$ ($E_{ox}^* = E_{ox} - E_{0\text{-}0}$). *d*) Driving forces for electron transfer processes. ΔG_{inj}: Driving forces for the electron injection from the singlet excited state (E_{ox}^*) of the dye to the TiO_2 conduction band (−0.5 V *vs*. NHE). ΔG_{reg}: Driving forces for the regeneration process of the dyes in the radical cation state (E_{ox}) by the I_3^-/I^- redox in the state of +0.4 V *vs*. NHE.

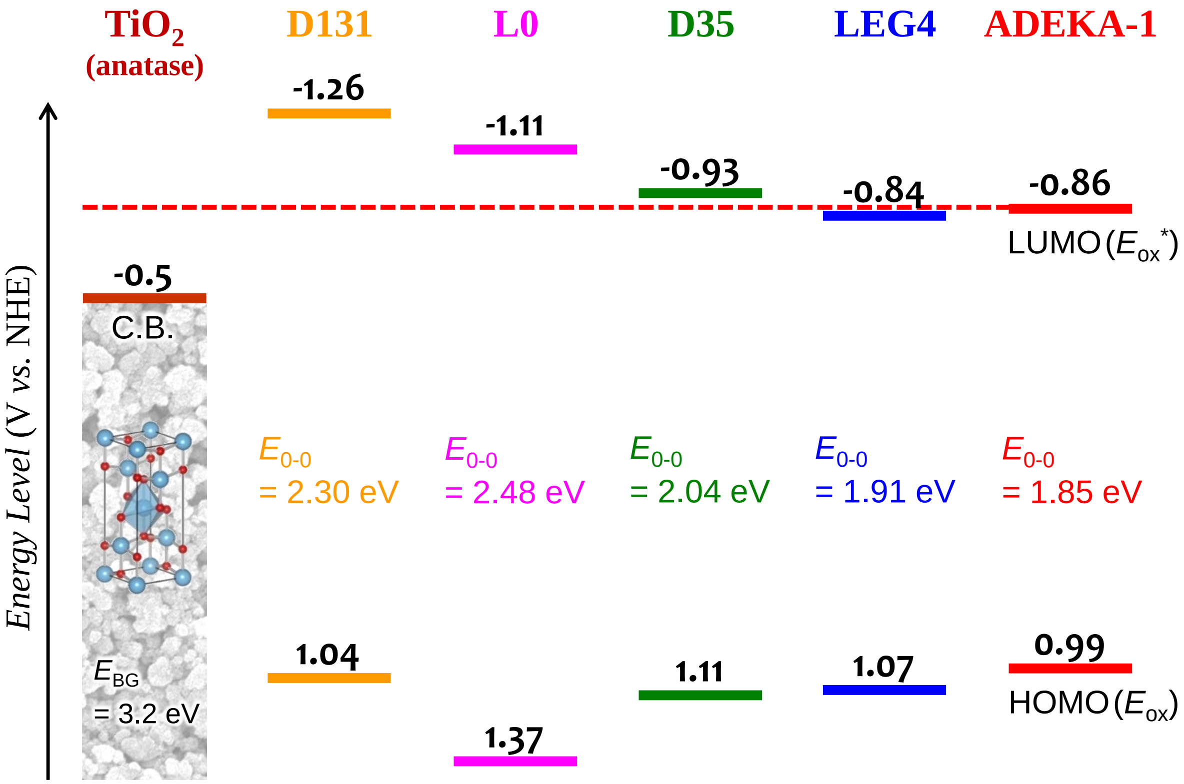

Figure S6. Energy levels of the frontier orbitals of **ADEKA-1** and the dyes employed as the co-photosensitizers in this work.[2,4,7,30]

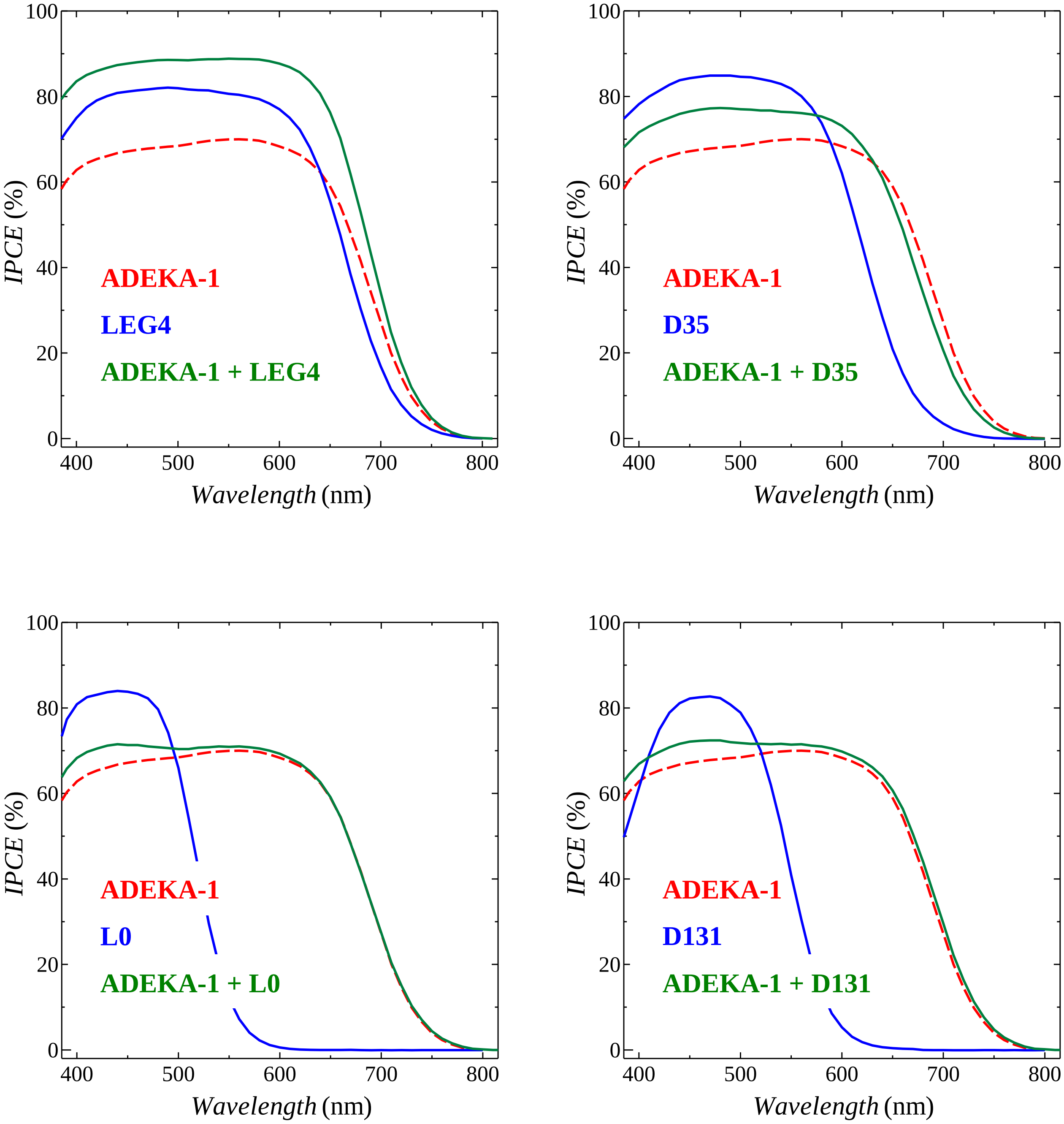

Figure S7. *IPCE* spectra of the cells photosensitized by **ADEKA-1** and/or **LEG4**, **D35**, **L0**, **D131** (Cell-A).

Table S2. Relative photovoltaic parameters of the cells photosensitized by **ADEKA-1** and/or **LEG4**, **D35**, **L0**, **D131** (Cell-A) under the illumination of the simulated sunlight (AM-1.5G, 100 mW cm^{-2}): short-circuit photocurrent density (J_{sc}), open-circuit photovoltage (V_{oc}), fill factor (FF) and light-to-electric energy conversion efficiency (η).

Dyes	Rel. J_{sc}	Rel. V_{oc}	Rel. FF	Rel. η
ADEKA-1	1.00	1.00	1.00	1.00
LEG4	1.04	0.79	0.89	0.73
D35	0.85	0.78	0.92	0.61
L0	0.52	0.72	1.02	0.38
D131	0.63	0.75	1.04	0.50
ADEKA-1 + **LEG4**	1.27	1.07	0.97	1.29
ADEKA-1 + **D35**	1.14	1.07	0.93	1.14
ADEKA-1 + **L0**	1.04	1.02	0.96	1.01
ADEKA-1 + **D131**	1.06	1.04	0.93	1.01

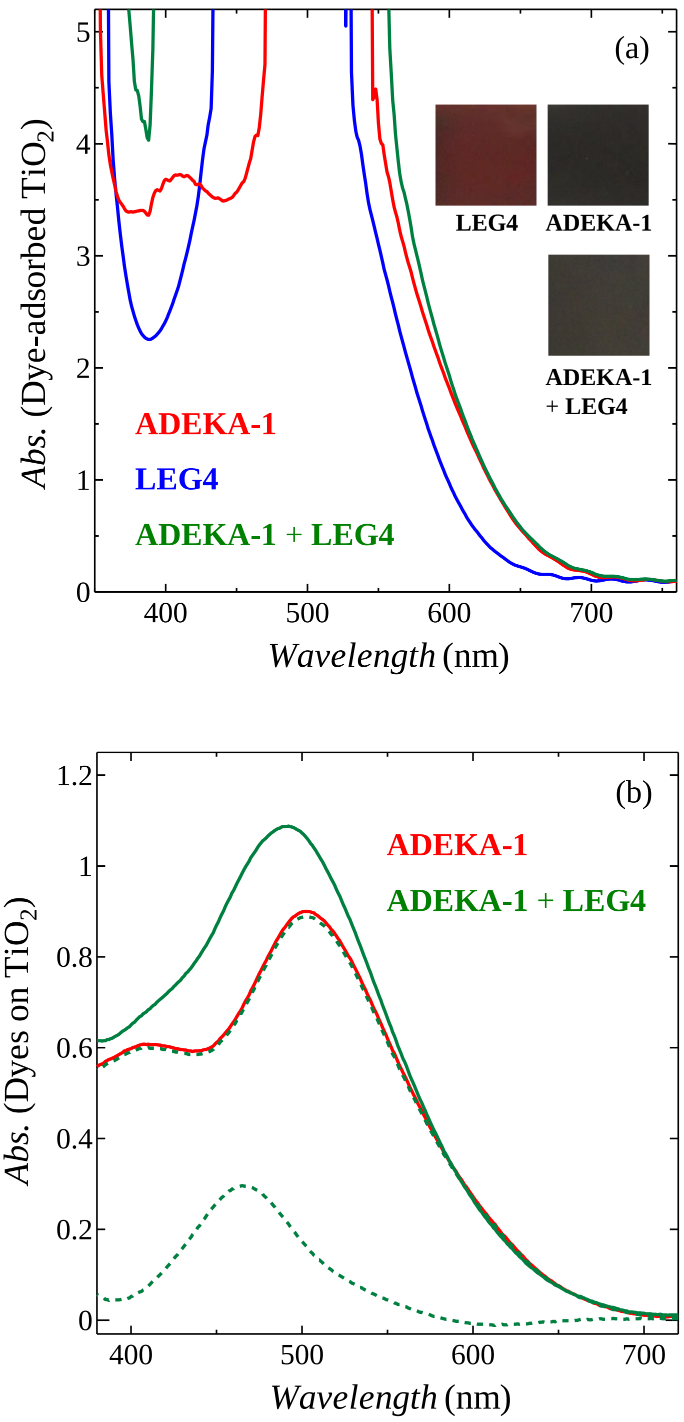

Figure S8. (a) Absorption spectra of **ADEKA-1**, **LEG4** and **ADEKA-1** + **LEG4** adsorbed TiO_2 electrodes (t ~ 4 μm). Insets show the photographs of the dye-adsorbed TiO_2 electrodes. (b) Absorption spectra in visible region of **ADEKA-1** and **ADEKA-1** + **LEG4** adsorbed on TiO_2 electrodes (t ~ 1 μm). Dotted lines represent the result of the spectral decomposition into the components by **ADEKA-1** and **LEG4**. The relative amount of the dyes adsorbed on the TiO_2 electrode was estimated to be 1.0 : 0.25 for **ADEKA-1** : **LEG4**.

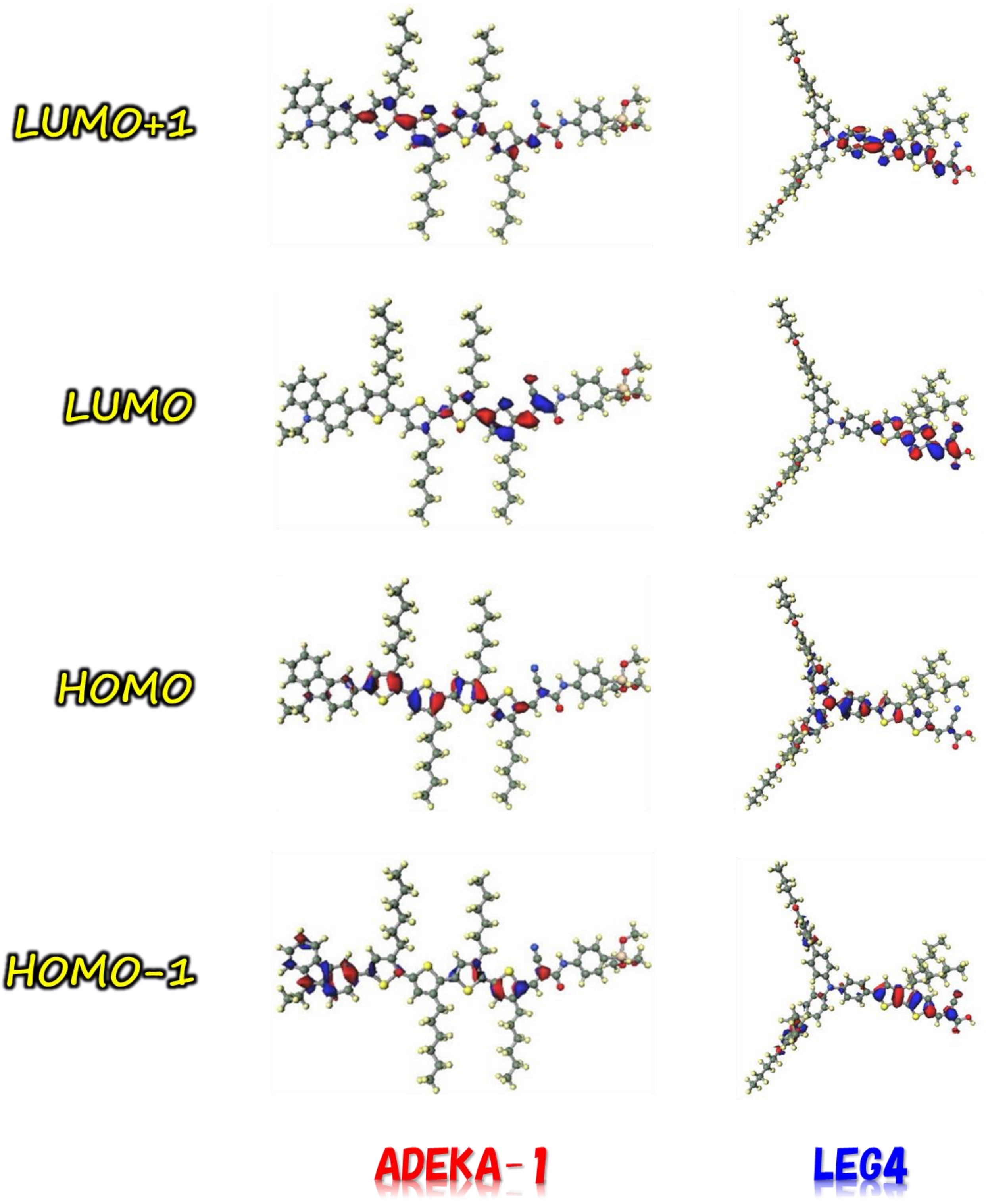

Figure S9. Molecular orbitals (HOMO-1, HOMO, LUMO and LUMO+1) of **ADEKA-1** and **LEG4** calculated by DFT at the CAM-B3LYP/6-31+G(d,p) // B3LYP/6-31+G(d,p) levels.

Table S3. Energy levels of HOMO-1, HOMO, LUMO and LUMO+1 for **ADEKA-1** and **LEG4** calculated by DFT at the CAM-B3LYP/6-31+G(d,p) // B3LYP/6-31+G(d,p) levels.

Dye	HOMO-1 (eV)	HOMO (eV)	LUMO (eV)	LUMO+1 (eV)
ADEKA-1	-6.8058	-6.1258	-1.8498	-0.3644
LEG4	-6.8643	-6.1528	-1.8994	-0.9138

Table S4. Calculated excited energies, oscillator strengths (*f*) and compositions in terms of molecular orbital contributions for **ADEKA-1** and **LEG4** (TDDFT: CAM-B3LYP/6-31+G(d,p) // B3LYP/6-31+G(d,p) levels).

Dye	State	Major Excitation (Coefficient : Contribution)*,**	Character	*Energy* (eV)	*f****
ADEKA-1	$S_0 \rightarrow S_1$	H → L (0.61865 : 77%) , H-1 → L (-0.23782 : 11%)	π-π^*	2.4504 (506.03 nm)	2.3502
	$S_0 \rightarrow S_2$	H → L+1 (0.52972 : 56%) , H-1 → L (-0.35061 : 25%)		3.2810 (377.93 nm)	0.1317
	$S_0 \rightarrow S_3$	H-1 → L (0.40218 : 32%) , H → L+1 (0.36720 : 27%)		3.7078 (334.43 nm)	0.0912
LEG4	$S_0 \rightarrow S_1$	H → L (0.56471 : 64%) , H-1 → L (0.36745 : 27%)	π-π^*	2.6147 (474.25 nm)	1.7820
		H-1 → L (0.48550 : 47%) , H → L (-0.28628 : 16%)		3.5037 (353.91 nm)	0.0240
	$S_0 \rightarrow S_2$	H → L+1 (0.53501 : 57%) , H → L (-0.27005 : 15%)		3.9280 (315.68 nm)	0.1954

*H = HOMO, L = LUMO

**|CI coeff.| > 0.1

***Oscillator strength [$4.319 \times 10^{-9} \cdot \int \varepsilon(\nu)\,d\nu$]

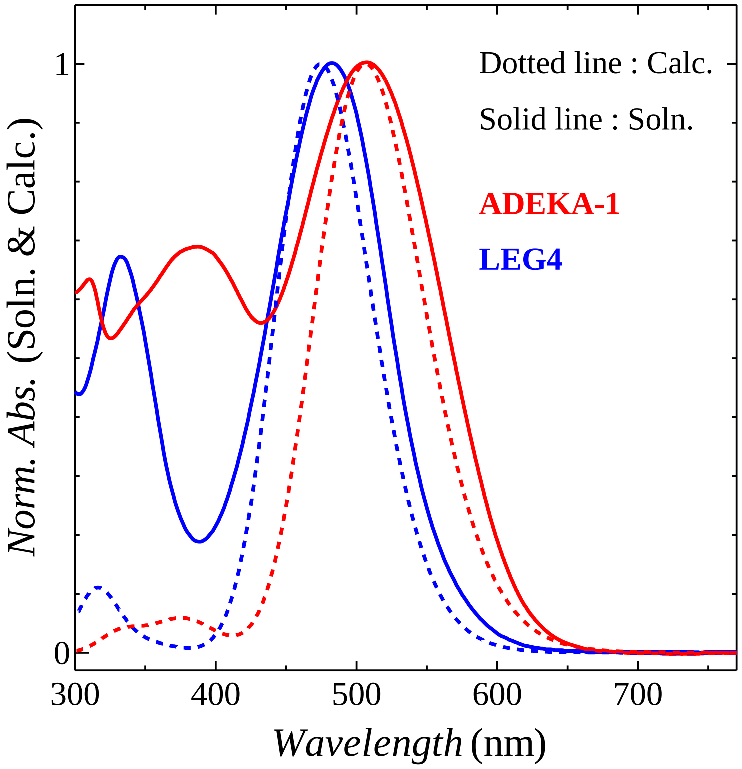

Figure S10. Calculated UV-visible absorption spectra (Dotted lines) of **ADEKA-1** and **LEG4** (TDDFT: CAM-B3LYP/6-31+G(d,p) // B3LYP/6-31+G(d,p) levels). All spectra were obtained by applying an artificial Gaussian broadening of 3,500 cm^{-1} FWHM to the intensities calculated with TDDFT for the visualization purpose. Solid lines show the experimental data of the dye solutions ($CHCl_3$ solution for **ADEKA-1** and EtOH solution for **LEG4**; Fig. S5).

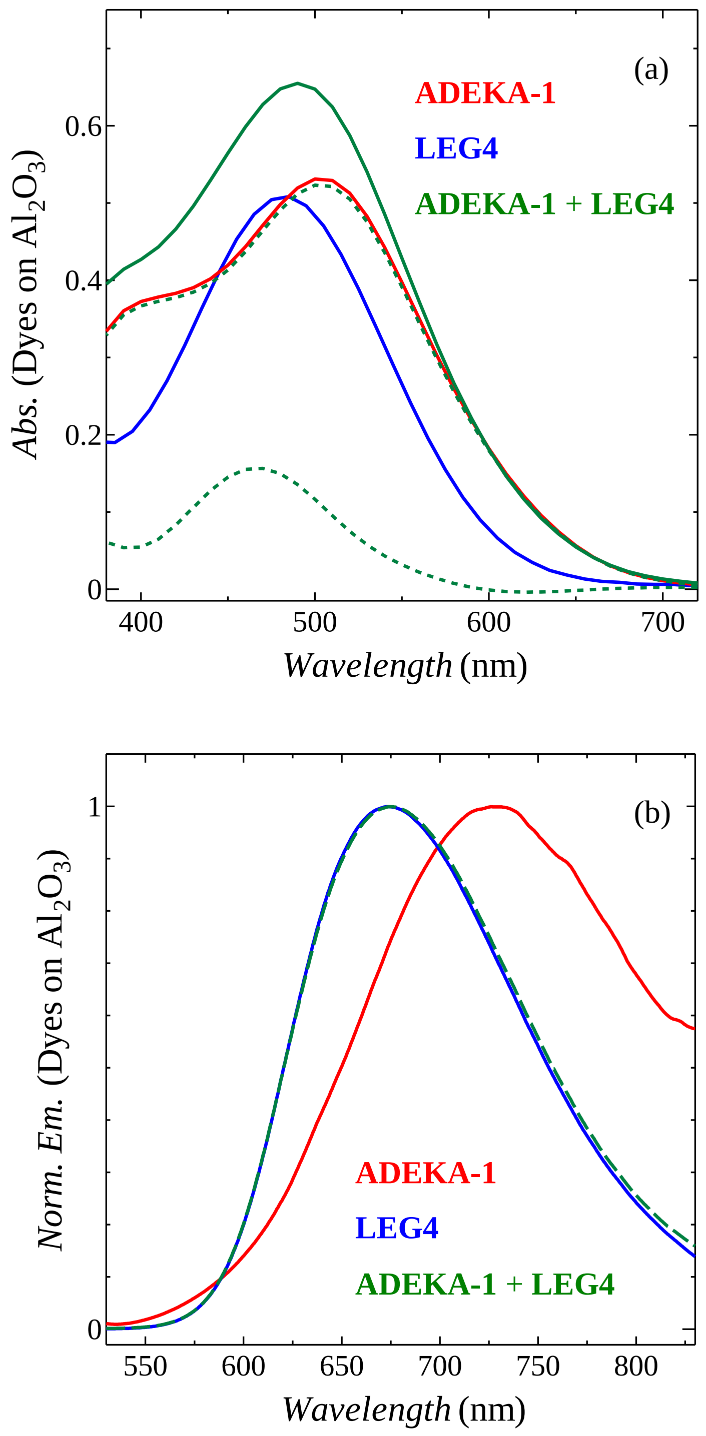

Figure S11. (a) Absorption spectra in visible region of **ADEKA-1**, **LEG4** and **ADEKA-1 + LEG4** adsorbed on Al_2O_3 porous films. Dotted lines represent the result of the spectral decomposition into the components by **ADEKA-1** and **LEG4**. The relative amount of the dyes adsorbed on the Al_2O_3 porous film was estimated to be 1.0 : 0.27 for **ADEKA-1** : **LEG4**. (b) Normalized emission spectra of the Al_2O_3 porous films modified by **ADEKA-1**, **LEG4** and **ADEKA-1 + LEG4**. The emission spectra were obtained by the excitation at 500 nm.

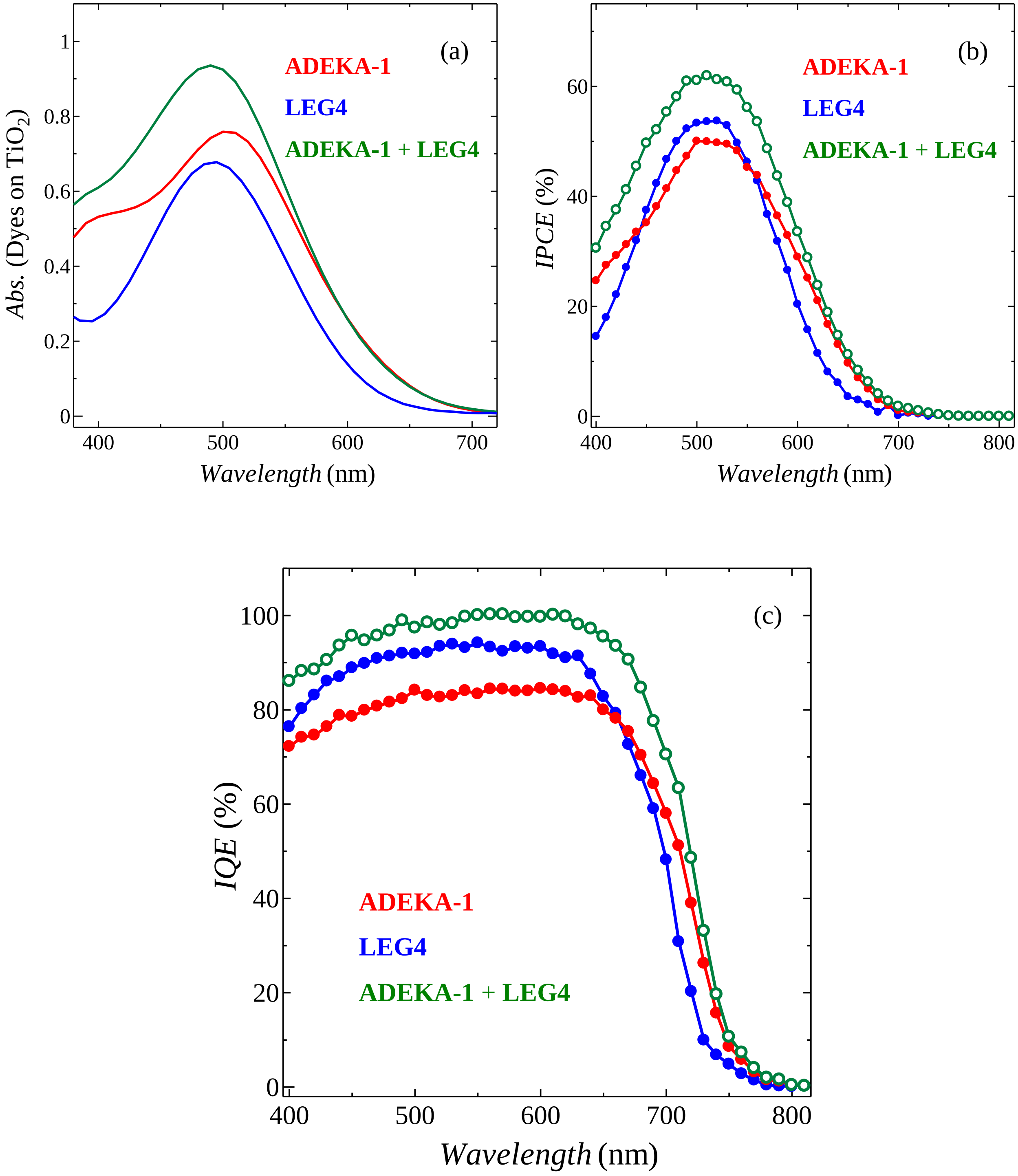

Figure S12. (a) Absorption spectra of the dyes adsorbed on the TiO_2 electrodes, (b) *IPCE* spectra of the cells used for the estimation of *IQE*s and (c) the estimated *IQE* spectra of the cells photosensitized by **ADEKA-1** and/or **LEG4**.

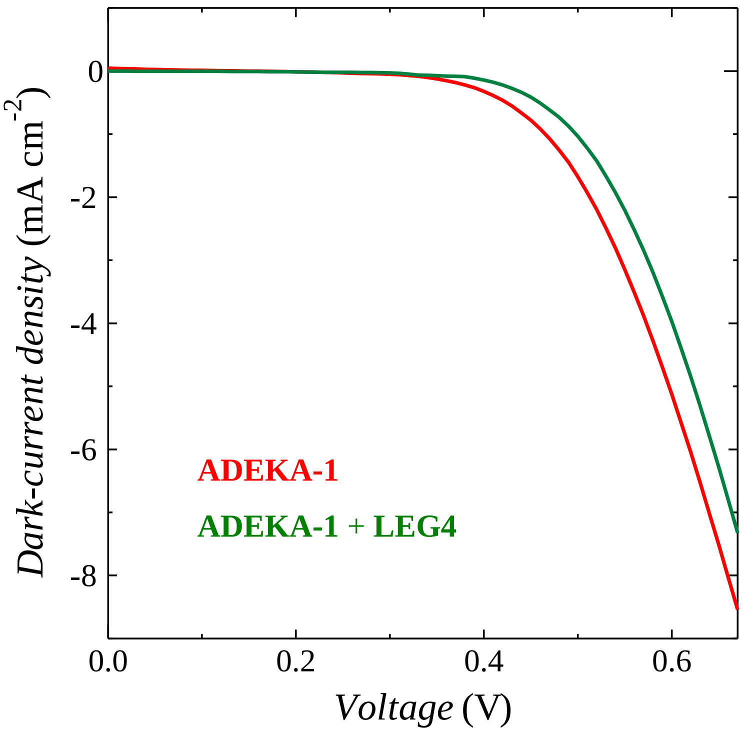

Figure S13. Dark *J*-*V* properties of the cells sensitized by **ADEKA-1** with/without **LEG4** (Cell-A).

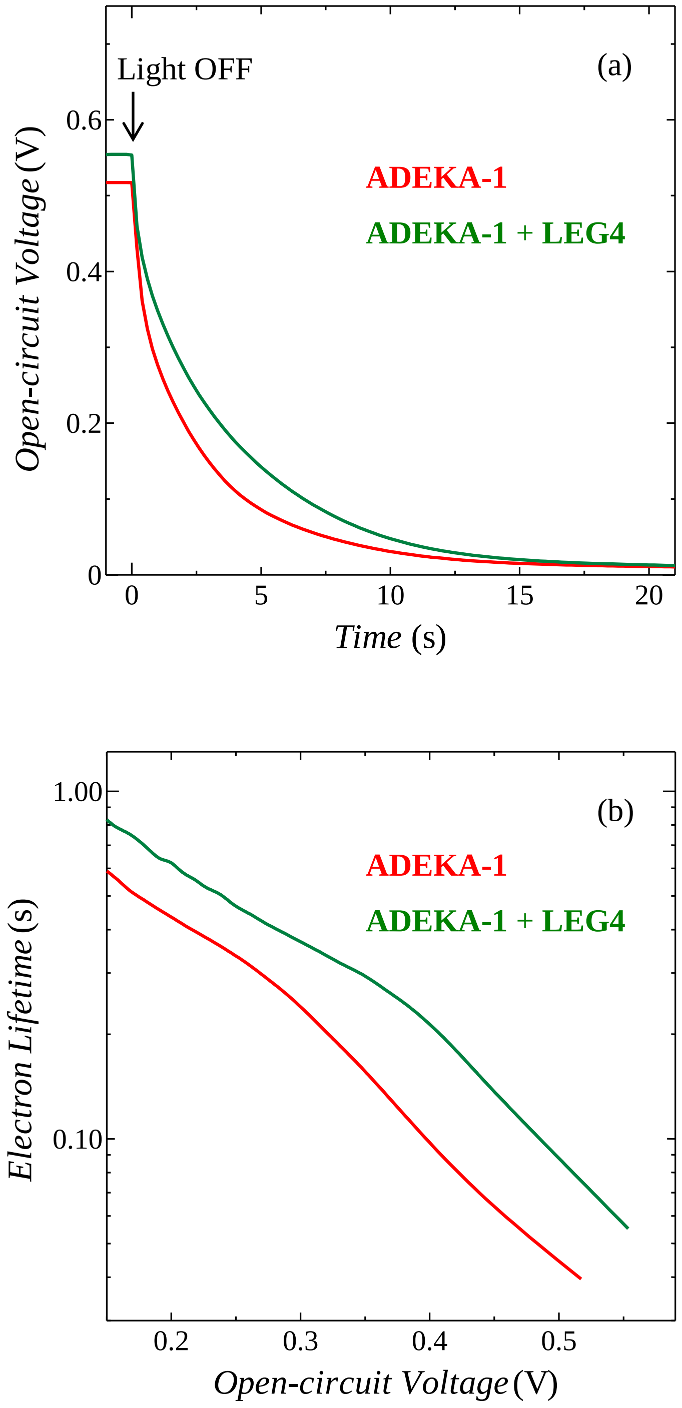

Figure S14. (a) Open-circuit voltage decays (OCVDs) of the cells photosensitized by **ADEKA-1** with/without **LEG4** (Cell-A). (b) Lifetime of the electrons in the TiO_2 conduction band plotted as a function of the open-circuit voltage.

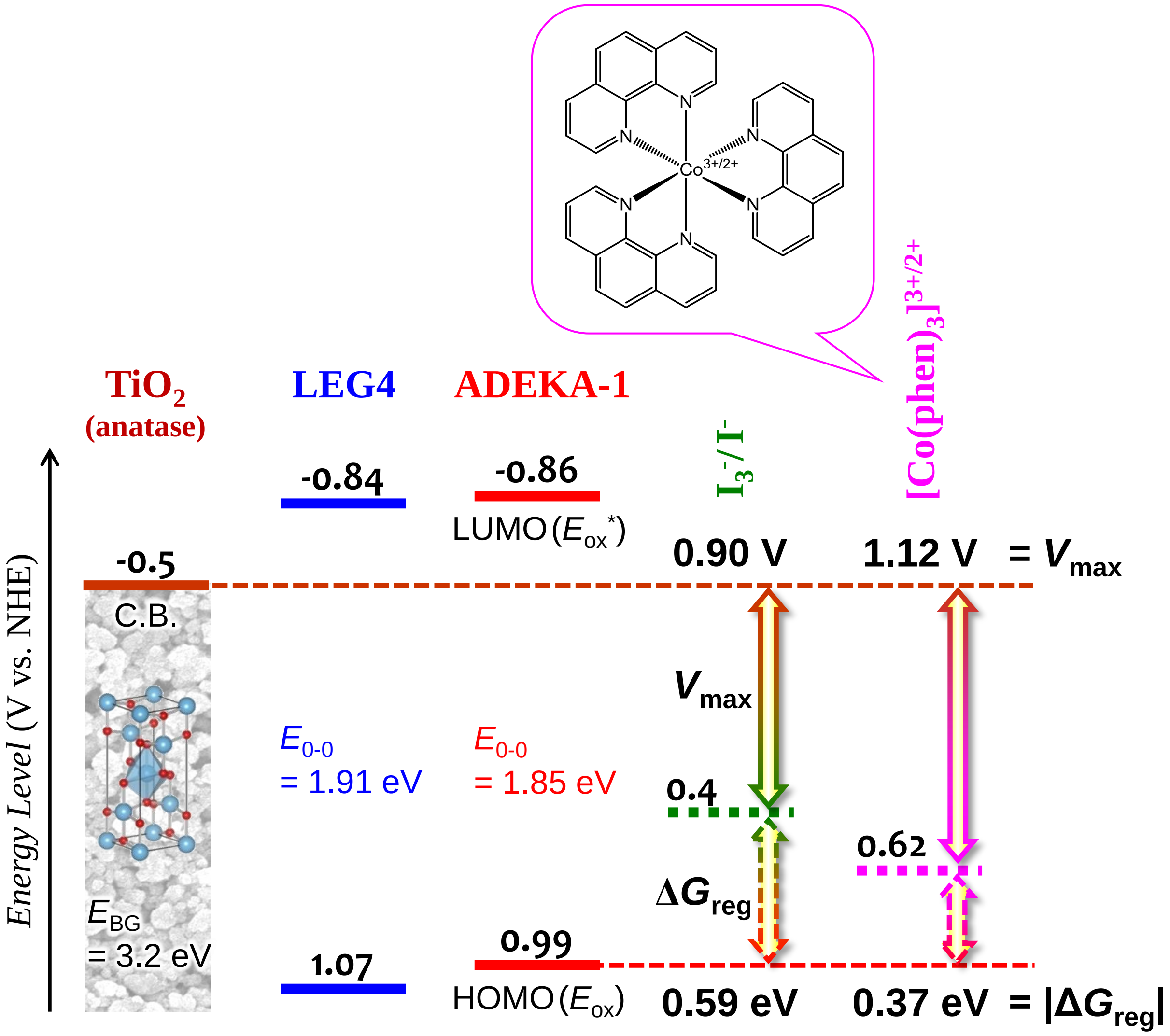

Figure S15. Schematic energy diagram of the DSSC composed of the anatase-TiO$_2$, the photosensitizing dyes of **ADEKA-1** and **LEG4**, and the redox electrolytes of I_3^-/I^- and $[Co(phen)_3]^{3+/2+}$ couples.[2,4,31] Molecular structure of the $[Co(phen)_3]^{3+/2+}$ is also shown.

Table S5. Photovoltaic parameters of the cells with the same composition as the best-performance cell of Entry 3 in Table 1; photosensitized collaboratively by **ADEKA-1** and **LEG4** using the $[Co(phen)_3]^{3+/2+}$ redox electrolyte (Electrolyte F) and the FTO/Au/GNP counter electrode under the illumination of the simulated sunlight (AM-1.5G, 100 mW cm^{-2}).

Entry	Dyes	Electrolyte : Redox	Counter Electrode	Light Intensity	J_{sc} (mA cm^{-2})	V_{oc} (V)	*FF*	η (%)
3a	**ADEKA-1** + **LEG4**	F : $[Co(phen)_3]^{3+/2+}$	FTO/Au/GNP	100 mW cm^{-2}	18.36	1.013	0.770	14.3
3b	**ADEKA-1** + **LEG4**	F : $[Co(phen)_3]^{3+/2+}$	FTO/Au/GNP	100 mW cm^{-2}	18.19	1.014	0.771	14.2
3c	**ADEKA-1** + **LEG4**	F : $[Co(phen)_3]^{3+/2+}$	FTO/Au/GNP	100 mW cm^{-2}	18.16	1.013	0.768	14.1
3d	**ADEKA-1** + **LEG4**	F : $[Co(phen)_3]^{3+/2+}$	FTO/Au/GNP	100 mW cm^{-2}	18.37	1.014	0.776	14.5
3 (Av.)	**ADEKA-1** + **LEG4**	F : $[Co(phen)_3]^{3+/2+}$	FTO/Au/GNP	100 mW cm^{-2}	18.27	1.014	0.771	14.3

Electrolyte: F) 0.20 M $[Co^{2+}(phen)_3](PF_6^-)_2$, 0.05 M $[Co^{3+}(phen)_3](PF_6^-)_3$, 0.07 M $LiClO_4$, 0.02 M $NaClO_4$, 0.03 M TBAPF, 0.01 M TBPPF, 0.01 M HMImPF, 0.30 M TBP, 0.10 M TMSP, 0.10 M MP, 0.05 M CPrBP, 0.10 M CPeBP, 0.05 M COcBP in MeCN.

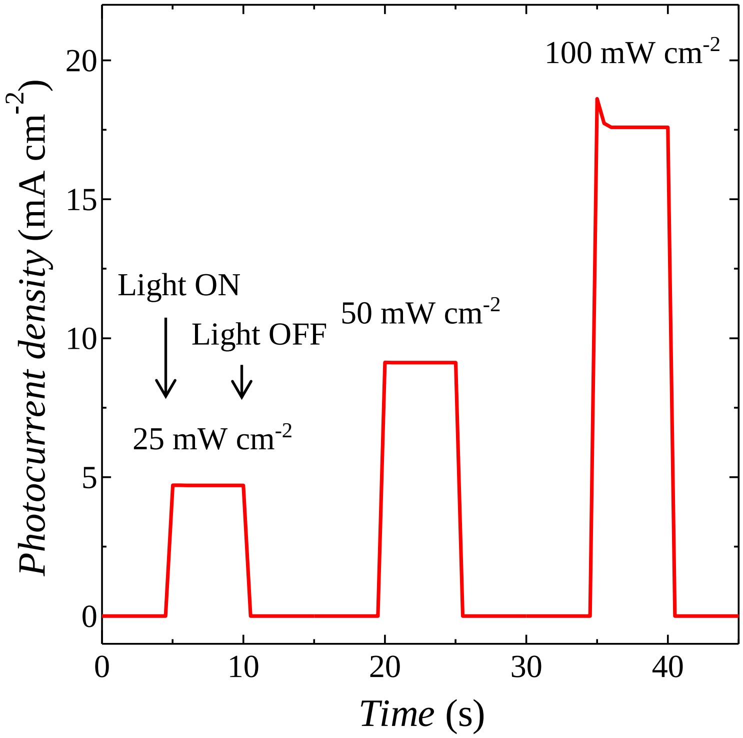

Figure S16. Photocurrent density transient dynamics of the cell photosensitized collaboratively by **ADEKA-1** and **LEG4** with the redox electrolyte containing $[Co(phen)_3]^{3+/2+}$ (Cell-B) at various simulated sunlight intensities. The initial decline of the photocurrent signal at the 100 mW cm^{-2} intensity would be due to a mass transfer limitation of $[Co(phen)_3]^{3+/2+}$.

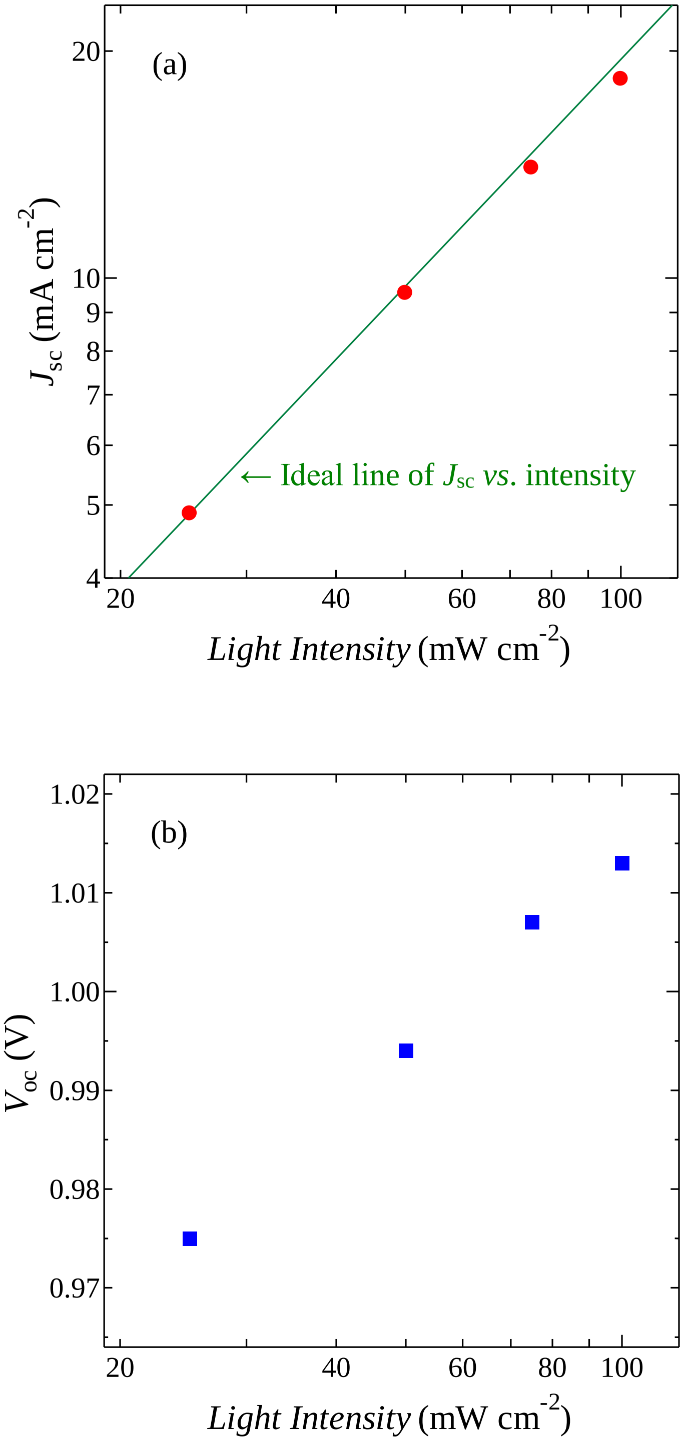

Figure S17. Dependences of the (a) J_{sc} and (b) V_{oc} on the light intensity for the best-performance cell photosensitized collaboratively by **ADEKA-1** and **LEG4** using the $[Co(phen)_3]^{3+/2+}$ redox electrolyte (Electrolyte F) and the FTO/Au/GNP counter electrode. The data include the results of Entries 3 and 4 in Table 1.

Table S6. Photovoltaic parameters of the cells photosensitized collaboratively by **ADEKA-1** and **LEG4** (Cell-B) under the illuminations of the simulated sunlight (AM-1.5G).

Entry	Dyes	Electrolyte : Redox	Counter Electrode	Light Intensity	J_{sc} (mA cm^{-2})	V_{oc} (V)	*FF*	η (%)
1	**ADEKA-1** + **LEG4**	A : I_3^-/I^-	FTO/Pt	100 mW cm^{-2}	19.11	0.783	0.748	11.2
S5	**ADEKA-1** + **LEG4**	B : $[\mathrm{Co(phen)_3}]^{3+/2+}$	FTO/Pt	100 mW cm^{-2}	17.62	0.969	0.761	13.0
S6	**ADEKA-1** + **LEG4**	C : $[\mathrm{Co(phen)_3}]^{3+/2+}$	FTO/Pt	100 mW cm^{-2}	18.08	0.963	0.760	13.2
S7	**ADEKA-1** + **LEG4**	D : $[\mathrm{Co(phen)_3}]^{3+/2+}$	FTO/Pt	100 mW cm^{-2}	17.66	0.957	0.759	12.8
S8	**ADEKA-1** + **LEG4**	E : $[\mathrm{Co(phen)_3}]^{3+/2+}$	FTO/Pt	100 mW cm^{-2}	17.43	1.007	0.764	13.4
2	**ADEKA-1** + **LEG4**	F : $[\mathrm{Co(phen)_3}]^{3+/2+}$	FTO/Pt	100 mW cm^{-2}	17.77	1.018	0.765	13.8
3a	**ADEKA-1** + **LEG4**	F : $[\mathrm{Co(phen)_3}]^{3+/2+}$	FTO/Au/GNP	100 mW cm^{-2}	18.36	1.013	0.770	14.3
4	**ADEKA-1** + **LEG4**	F : $[\mathrm{Co(phen)_3}]^{3+/2+}$	FTO/Au/GNP	50 mW cm^{-2}	9.55	0.994	0.776	14.7

Electrolyte: A) 0.07 M I_2, 0.05 M LiI, 0.05 M NaI, 0.50 M DMPImI, 0.10 M EMImI, 0.05 M TBAI, 0.05 M THAI, 0.40 M TBP, 0.10 M MP, 0.10 M GuSCN in MeCN/VN/THF (8:1:1 in volume).
Electrolyte: B) 0.25 M $[\mathrm{Co^{2+}(phen)_3}](\mathrm{PF_6^-})_2$, 0.035 M $[\mathrm{Co^{3+}(phen)_3}](\mathrm{PF_6^-})_3$, 0.10 M $\mathrm{LiClO_4}$, 0.50 M TBP in MeCN.
Electrolyte: C) 0.20 M $[\mathrm{Co^{2+}(phen)_3}](\mathrm{PF_6^-})_2$, 0.05 M $[\mathrm{Co^{3+}(phen)_3}](\mathrm{PF_6^-})_3$, 0.10 M $\mathrm{LiClO_4}$, 0.50 M TBP in MeCN.
Electrolyte: D) 0.20 M $[\mathrm{Co^{2+}(phen)_3}](\mathrm{TFSI})_2$, 0.05 M $[\mathrm{Co^{3+}(phen)_3}](\mathrm{TFSI})_3$, 0.10 M $\mathrm{LiClO_4}$, 0.50 M TBP in MeCN.
Electrolyte: E) 0.20 M $[\mathrm{Co^{2+}(phen)_3}](\mathrm{PF_6^-})_2$, 0.05 M $[\mathrm{Co^{3+}(phen)_3}](\mathrm{PF_6^-})_3$, 0.07 M $\mathrm{LiClO_4}$, 0.02 M $\mathrm{NaClO_4}$, 0.03 M TBAPF, 0.01 M TBPPF, 0.01 M HMImPF, 0.30 M TBP, 0.10 M TMSP, 0.10 M MP in MeCN.
Electrolyte: F) 0.20 M $[\mathrm{Co^{2+}(phen)_3}](\mathrm{PF_6^-})_2$, 0.05 M $[\mathrm{Co^{3+}(phen)_3}](\mathrm{PF_6^-})_3$, 0.07 M $\mathrm{LiClO_4}$, 0.02 M $\mathrm{NaClO_4}$, 0.03 M TBAPF, 0.01 M TBPPF, 0.01 M HMImPF, 0.30 M TBP, 0.10 M TMSP, 0.10 M MP, 0.05 M CPrBP, 0.10 M CPeBP, 0.05 M COcBP in MeCN.

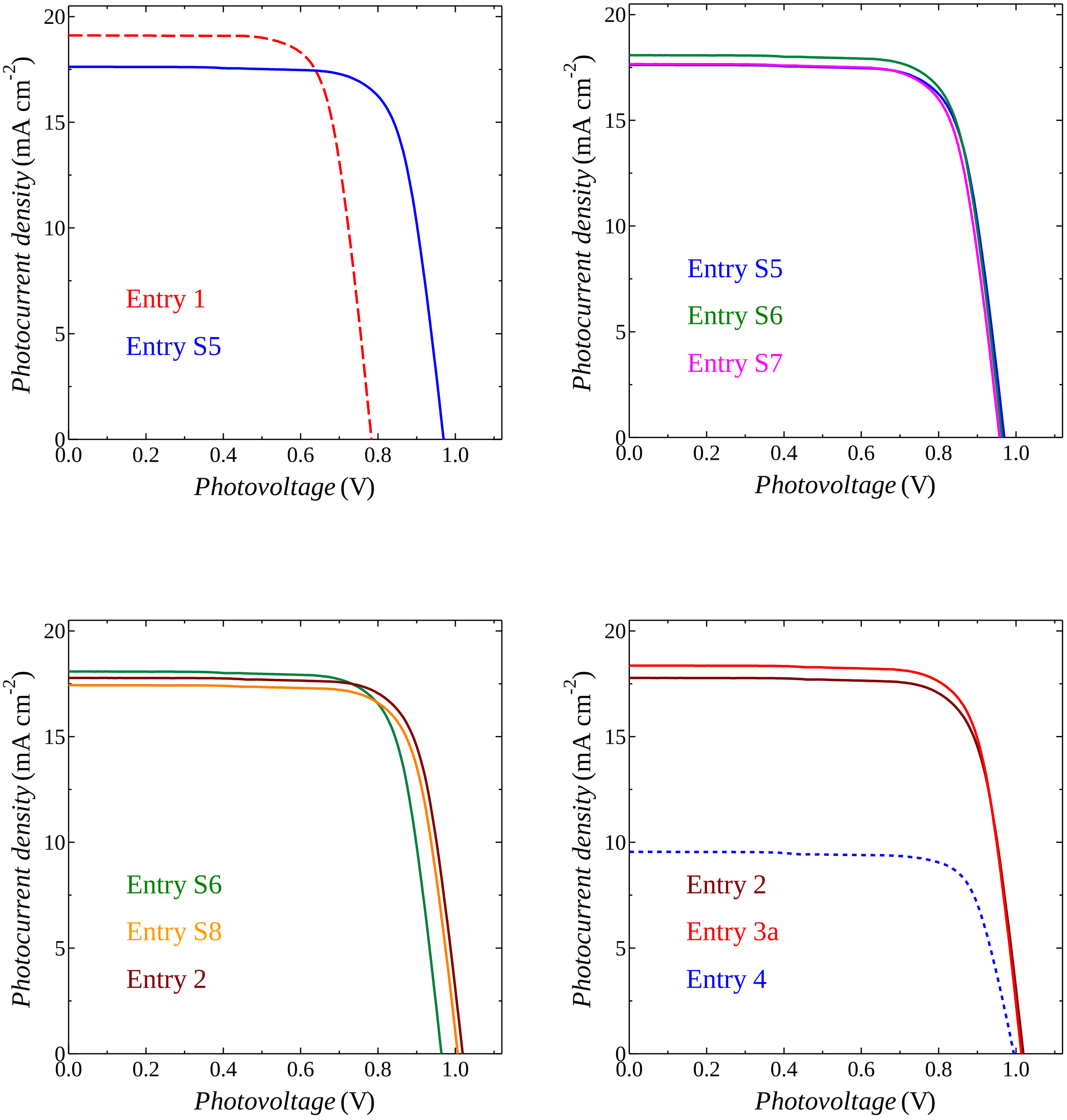

Figure S18. *J*-*V* properties of the cells photosensitized collaboratively by **ADEKA-1** and **LEG4** (Cell-B) using I_3^-/I^- and $Co^{3+/2+}$ redox electrolytes under the illumination of the simulated sunlight (AM-1.5G, 100 mW cm^{-2} and 50 mW cm^{-2} only for Entry 4). The entry numbers correspond to those in Tables 1 and S6.

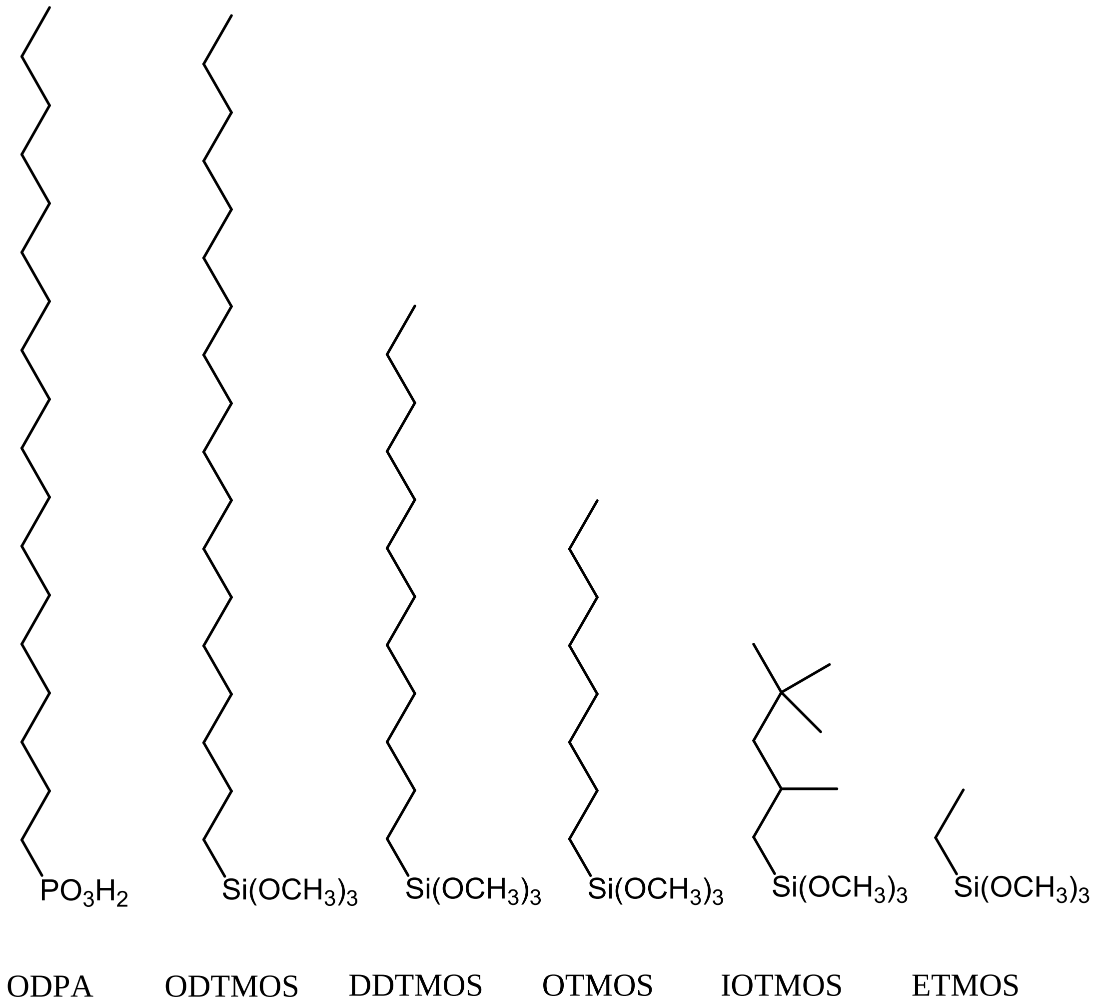

Figure S19. Molecular structures of alkyl compounds with anchor-moieties (octadecylphosphonic acid: ODPA, octadecyltrimethoxysilane: ODTMOS, dodecyltrimethoxysilane: DDTMOS, octyltrimethoxysilane: OTMOS, isooctyltrimethoxysilane: IOTMOS and ethyltrimethoxysilane: ETMOS) used in the hierarchical multi-capping treatment.

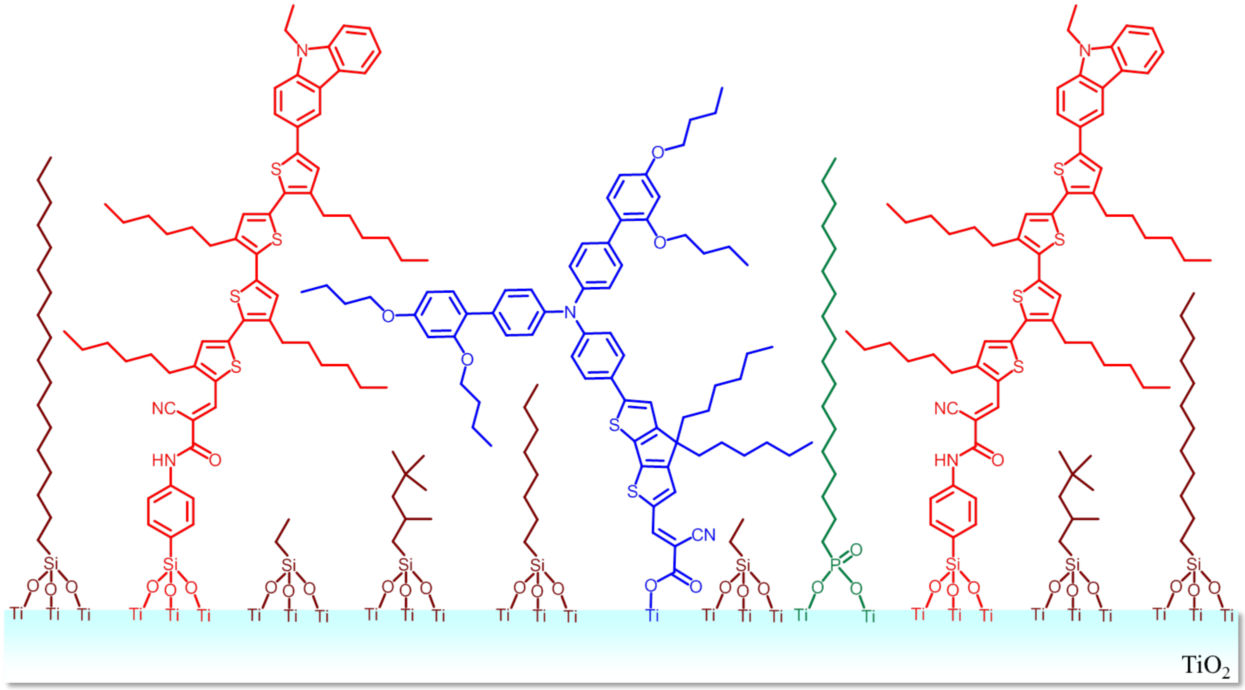

Figure S20. Schematic drawing of the ‘alkyl-thicket’ structure on the **ADEKA-1** + **LEG4**-co-adsorbed TiO_2 photoelectrode formed by the hierarchical multi-capping treatment.

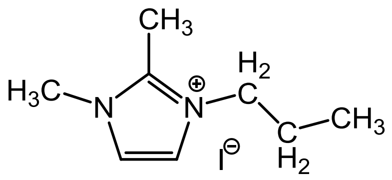

DMPImI

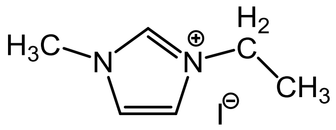

EMImI

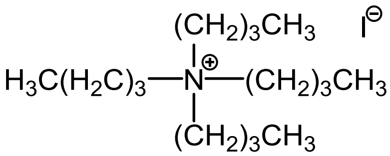

TBAI

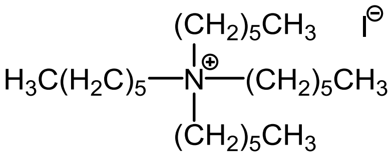

THAI

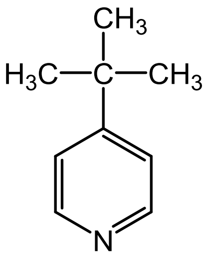

TBP

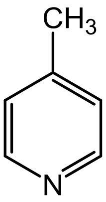

MP

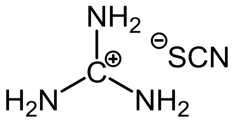

GuSCN

Figure S21. Molecular structures of additives (1,2-dimethyl-3-*n*-propylimidazolium iodide: DMPImI, 1-ethyl-3-methylimidazolium iodide: EMImI, tetra-*n*-butylammonium iodide: TBAI, tetra-*n*-hexylammonium iodide: THAI, 4-*tert*-butylpyridine: TBP, 4-methylpyridine: MP and guanidinium thiocyanate: GuSCN) used in the I_3^-/I^- redox electrolyte (Electrolyte A).

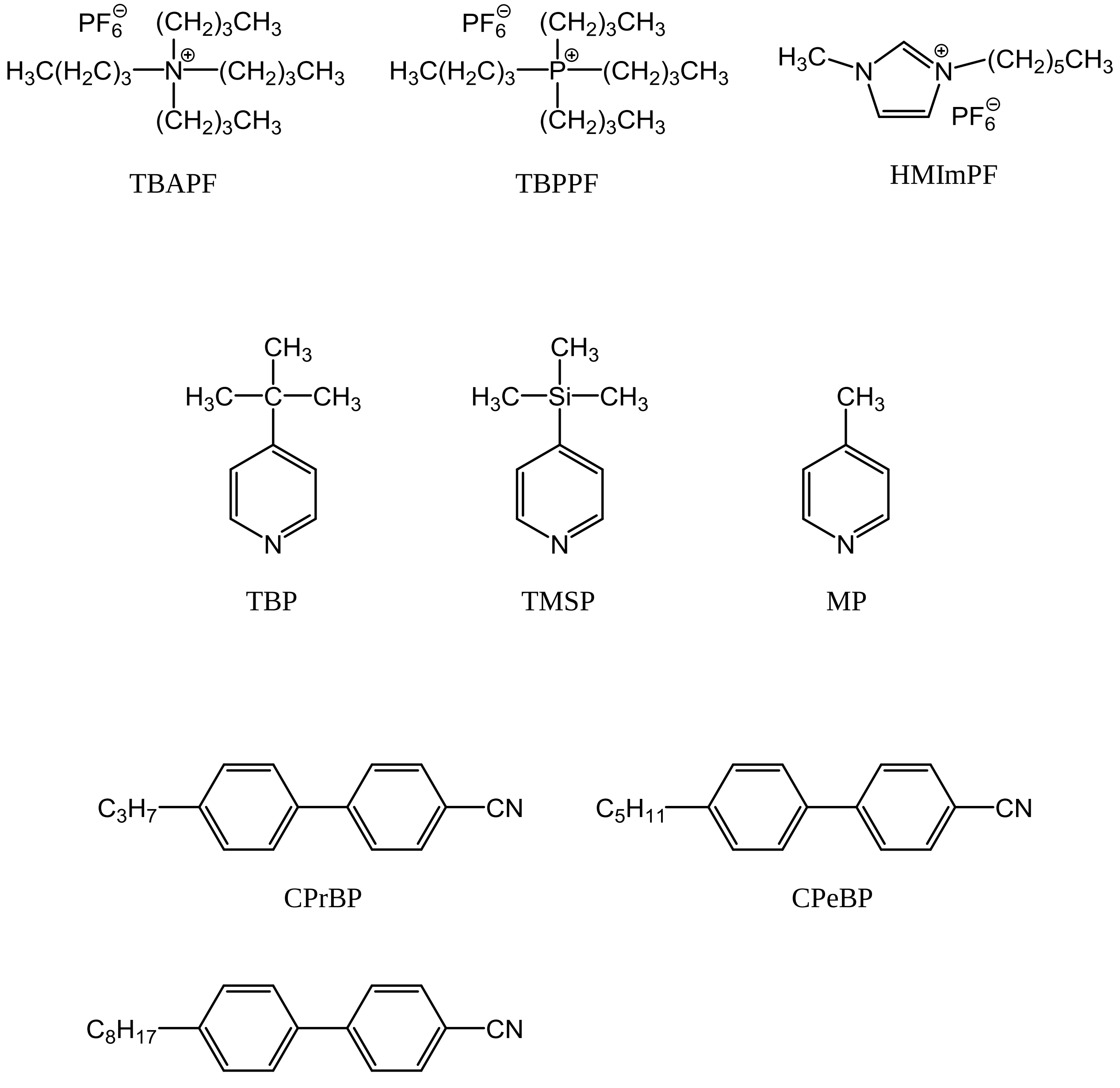
TBAPF TBPPF HMImPF

TBP TMSP MP

CPrBP CPeBP

COcBP

Figure S22. Molecular structures of additives (tetrabutylammonium hexafluorophosphate: TBAPF, tetrabutylphosphonium hexafluorophosphate: TBPPF, 1-hexyl-3-methylimidazolium hexafluorophosphate: HMImPF, 4-*tert*-butylpyridine: TBP, 4-trimethylsilylpyridine: TMSP, 4-methylpyridine: MP, 4-cyano-4'-propylbiphenyl: CPrBP, 4-cyano-4'-pentylbiphenyl: CPeBP and 4-cyano-4'-octylbiphenyl: COcBP) used in the cobalt(III/II) complex redox electrolytes (Electrolytes B-F).

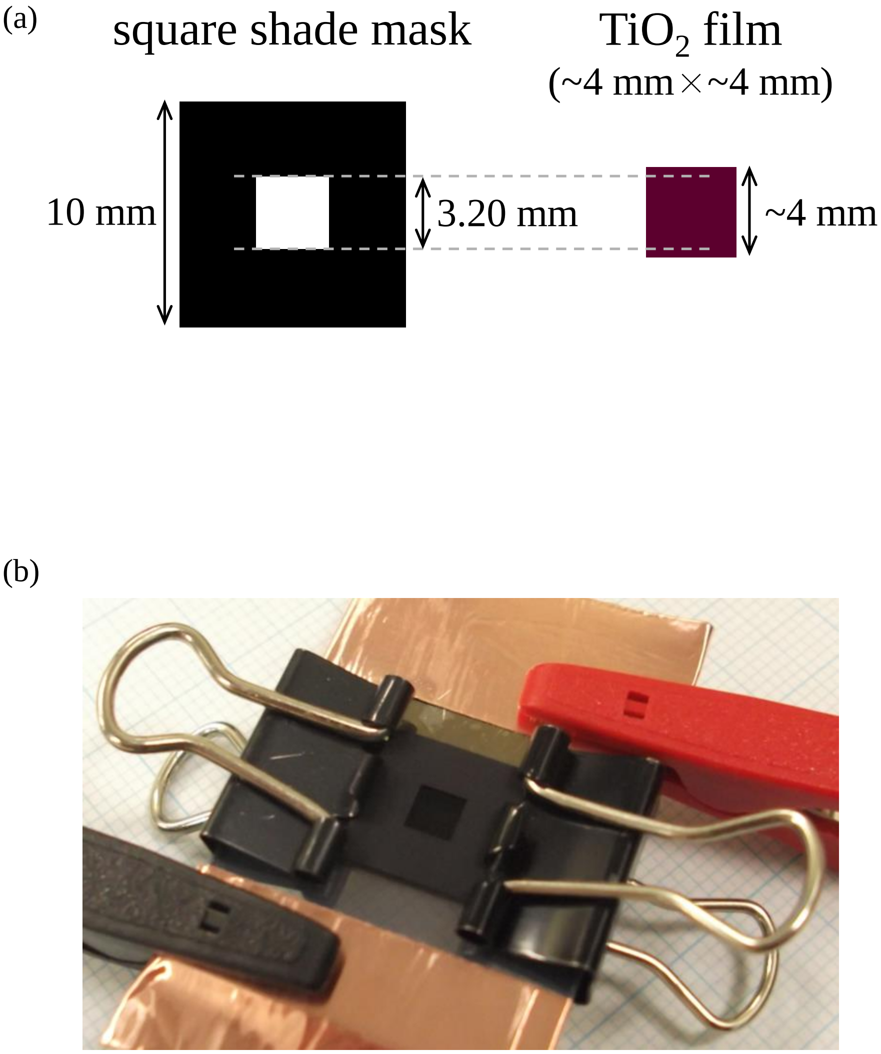

Figure S23. (a) Schematic drawing for size of the square black shade mask and the TiO$_2$ porous film with the photosensitizing dyes. (b) Photograph of the electrochemical cell of the open sandwich type used in this work (Cell-B). In the photovoltaic measurements, the spaces between the shade mask and the Cu conduction tapes were also shaded to avoid light scatter and other undesirable effects producing uncertainties in the measurements.

References (Electronic Supplementary Information)

1. Z.-S. Wang, N. Koumura, Y. Cui, M. Takahashi, H. Sekiguchi, A. Mori, T. Kubo, A. Furube and K. Hara, *Chem. Mater.*, 2008, **20**, 3993.
2. K. Kakiage, Y. Aoyama, T. Yano, T. Otsuka, T. Kyomen, M. Unno and M. Hanaya, *Chem. Commun.*, 2014, **50**, 6379.
3. K. Kakiage, Y. Aoyama, T. Yano, K. Oya, T. Kyomen and M. Hanaya, *Chem. Commun.*, 2015, **51**, 6315.
4. H. Ellis, S. K. Eriksson, S. M. Feldt, E. Gabrielsson, P. W. Lohse, R. Lindblad, L. Sun, H. Rensmo, G. Boschloo and A. Hagfeldt, *J. Phys. Chem. C*, 2013, **117**, 21029.
5. E. Gabrielsson, H. Ellis, S. Feldt, H. Tian, G. Boschloo, A. Hagfeldt and L. Sun, *Adv. Energy Mater.*, 2013, **3**, 1647.
6. D. P. Hagberg, X. Jiang, E. Gabrielsson, M. Linder, T. Marinado, T. Brinck, A. Hagfeldt and L. Sun, *J. Mater. Chem.*, 2009, **19**, 7232.
7. T. Kitamura, M. Ikeda, K. Shigaki, T. Inoue, N. A. Anderson, X. Ai, T. Lian and S. Yanagida, *Chem. Mater.*, 2004, **16**, 1806.
8. W. H. Howie, F. Claeyssens, H. Miura and L. M. Peter, *J. Am. Chem. Soc.*, 2008, **130**, 1367.
9. T. Koyanagi, A. Tanaka, M. Hashimoto, H. Miya and T. Mizuno, *JGC Technical Journal*, 2013, **1**, No. 7.
10. S. Ito, T. N. Murakami, P. Comte, P. Liska, C. Grätzel, M. K. Nazeeruddin and M. Grätzel, *Thin Solid Films*, 2008, **516**, 4613.
11. J. Xia and S. Yanagida, *Solar Energy*, 2011, **85**, 3143.
12. H. Ozawa, Y. Okuyama and H. Arakawa, *Dalton Trans.*, 2012, **41**, 5137.
13. S. Ito, P. Chen, P. Comte, M. K. Nazeeruddin, P. Liska, P. Péchy and M. Grätzel, *Prog. Photovolt: Res. Appl.*, 2007, **15**, 603.
14. J. Yang, P. Ganesan, J. Teuscher, T. Moehl, Y. J. Kim, C. Yi, P. Comte, K. Pei, T. W. Holcombe, M. K. Nazeeruddin, J. Hua, S. M. Zakeeruddin, H. Tian and M. Grätzel, *J. Am. Chem. Soc.*, 2014, **136**, 5722.
15. S. Mathew, A. Yella, P. Gao, R. Humphry-Baker, B. F. E. Curchod, N. Ashari-Astani, I. Tavernelli, U. Rothlisberger, M. K. Nazeeruddin and M. Grätzel, *Nat. Chem.*, 2014, **6**, 242.
16. T. Kanzaki, S. Nakade, Y. Wada and S. Yanagida, *Photochem. Photobiol. Sci.*, 2006, **5**, 389.
17. S. Zhang, X. Yang, K. Zhang, H. Chen, M. Yanagida and L. Han, *Phys. Chem. Chem. Phys.*, 2011, **13**, 19310.
18. C. Zhang, Y. Huang, Z. Huo, S. Chen and S. Dai, *J. Phys. Chem. C*, 2009, **113**, 21779.
19. A. Fukui, R. Komiya, R. Yamanaka, A. Islam and L. Han, *Sol. Energy Mater. Sol. Cells*, 2006, **90**, 649.
20. X. Zong, M. Liang, C. Fan, K. Tang, G. Li, Z. Sun and S. Xue, *J. Phys. Chem. C*, 2012, **116**, 11241.

21. K. Kakiage, T. Tsukahara, T. Kyomen, M. Unno and M. Hanaya, *Chem. Lett.*, 2012, **41**, 895.

22. T. M. Koh, H. Li, K. Nonomura, N. Mathews, A. Hagfeldt, M. Grätzel, S. G. Mhaisalkar and A. C. Grimsdale, *Chem. Commun.*, 2013, **49**, 9101.

23. Gaussian 09, Revision D.01, M. J. Frisch, G. W. Trucks, H. B. Schlegel, G. E. Scuseria, M. A. Robb, J. R. Cheeseman, G. Scalmani, V. Barone, B. Mennucci, G. A. Petersson, H. Nakatsuji, M. Caricato, X. Li, H. P. Hratchian, A. F. Izmaylov, J. Bloino, G. Zheng, J. L. Sonnenberg, M. Hada, M. Ehara, K. Toyota, R. Fukuda, J. Hasegawa, M. Ishida, T. Nakajima, Y. Honda, O. Kitao, H. Nakai, T. Vreven, J. A. Montgomery, Jr., J. E. Peralta, F. Ogliaro, M. Bearpark, J. J. Heyd, E. Brothers, K. N. Kudin, V. N. Staroverov, R. Kobayashi, J. Normand, K. Raghavachari, A. Rendell, J. C. Burant, S. S. Iyengar, J. Tomasi, M. Cossi, N. Rega, J. M. Millam, M. Klene, J. E. Knox, J. B. Cross, V. Bakken, C. Adamo, J. Jaramillo, R. Gomperts, R. E. Stratmann, O. Yazyev, A. J. Austin, R. Cammi, C. Pomelli, J. W. Ochterski, R. L. Martin, K. Morokuma, V. G. Zakrzewski, G. A. Voth, P. Salvador, J. J. Dannenberg, S. Dapprich, A. D. Daniels, Ö. Farkas, J. B. Foresman, J. V. Ortiz, J. Cioslowski and D. J. Fox, Gaussian, Inc., Wallingford CT, 2009.

24. C. Lee, W. Yang and R. G. Parr, *Phys. Rev. B*, 1988, **37**, 785.

25. A. D. Becke, *J. Chem. Phys.*, 1993, **98**, 5648.

26. T. Yanai, D. P. Tew and N. C. Handy, *Chem. Phys. Lett.*, 2004, **393**, 51.

27. C. A. Ullrich, *Time-Dependent Density-Functional Theory: Concepts and Applications*, Oxford University Press, 2012.

28. H. Imahori, H. Norieda, H. Yamada, Y. Nishimura, I. Yamazaki, Y. Sakata and S. Fukuzumi, *J. Am. Chem. Soc.*, 2001, **123**, 100.

29. A. Zaban, M. Greenshtein and J. Bisquert, *ChemPhysChem*, 2003, **4**, 859.

30. T. Dentani, Y. Kubota, K. Funabiki, J. Jin, T. Yoshida, H. Minoura, H. Miura and M. Matsui, *New J. Chem.*, 2009, **33**, 93.

31. S. M. Feldt, G. Wang, G. Boschloo and A. Hagfeldt, *J. Phys. Chem. C*, 2011, **115**, 21500.

Acknowledgements

This work was partly supported by the “*Element Innovation*” Project by Ministry of Education, Culture, Sports, Science & Technology in Japan and by JSPS KAKENHI Grant Number 15H03848.